Growth and reproductive rates of the dominant copepod *Pseudodiaptomus forbesi* in response to environmental factors and habitat type in the northern San Francisco Estuary

Austin J. Gearty · Toni R. Ignoffo · Anne M. Slaughter · Wim J. Kimmerer

Abstract We examined growth and egg production rates of *Pseudodiaptomus forbesi* (*Copepoda*: *Calanoida*) in the northern San Francisco Estuary (SFE), California, USA. Data from several earlier studies were combined with new data to assess the responses of these vital rates to environmental factors. We measured 118 growth rates of early copepodites (C1–C3) and 191 egg production rates (EPRs) during spring–autumn of 10 years between 2006 and 2018. Samples were taken from four habitat types: brackish open water, fresh open water, wetland, and tidal channel. Growth rates averaged 0.21 d^{-1} (range 0–0.53 d^{-1}), while EPR averaged 2.4 eggs $♀^{-1}$ d^{-1} (range 0–11 eggs $♀^{-1}$ d^{-1}). Mass-specific EPR of females averaged about 20% of copepodite growth rate, meaning that specific egg production rate is not a suitable proxy for specific growth rate of this species. A rectangular hyperbola predicted 24% of the variation in growth rate from chlorophyll concentration and 19% of the variation in EPR (28% with habitat type as a covariate). Most of the chlorophyll values were below levels where growth rate or EPR approach their maxima. Lipid composition in a subset of samples gave no better prediction of growth rate than chlorophyll and was unrelated to EPR. Growth and reproduction of *P. forbesi* were food-limited most of the time, particularly in the open-water habitats. Despite high variability, these measurements make clear that the chronically low primary production in the northern SFE imposes limits on the food web supporting declining fish populations.

Keywords *Pseudodiaptomus forbesi* · Copepod · Growth rate · Egg production rate · Chlorophyll *a* · Estuaries

Handling Editor: Télesphore Sime-Ngando.

A. J. Gearty · T. R. Ignoffo · A. M. Slaughter · W. J. Kimmerer (✉)
Estuary and Ocean Science Center, San Francisco State University, 3150 Paradise Drive, Tiburon, CA 94920, USA
e-mail: kimmerer@sfsu.edu

Introduction

Understanding the responses of copepod productivity to fluctuations in available food resources is a key objective of copepod ecology. Copepod productivity can be represented by specific growth rate—the rate at which consumed organic matter is converted to mass of nauplii or copepodites—or by mass-specific egg production of adult females. Growth rate estimates are labor-intensive and enlist several widely used methods, each requiring various assumptions (Kobari et al.

2019). Egg production rate (EPR) estimates, in contrast, can be obtained through brief experiments (White and Roman 1992) or by the egg-ratio method for sac-spawning species (Edmondson et al. 1962). Measurements of copepod growth and reproductive rates provide information on energy flow and secondary production and are key components of population dynamics.

If growth rate and weight-specific egg production rate (SEPR) were equivalent measures of copepod growth, researchers could estimate the parameters of copepod production using relatively inexpensive measurements of egg production (Runge and Roff 2000). Corkett and McLaren (1978) and Sekiguchi et al. (1980) determined that SEPRs of *Pseudocalanus* spp. and *Acartia hudsonica*, respectively, were equivalent to growth rates of copepodites with saturating food concentrations. This equivalence has been extended to food-limited conditions in laboratory experiments (Berggreen et al. 1988), but several field investigations have found growth and SEPR to be divergent (Peterson et al. 1991; Richardson and Verheye 1998; Calbet et al. 2000), especially where copepods are food limited (Hirst and Bunker 2003).

Growth and reproduction of copepods are often food limited in oceanic, coastal, and estuarine environments (Kleppel et al. 1996; Kimmel 2012). Hirst and Bunker (2003) assembled growth rates and SEPR from a large number of studies and modeled the relationships of these vital rates to temperature, body weight, and food indices (primarily chlorophyll *a*). These analyses included mostly broadcast spawners that shed their eggs freely into the water column. Fewer data were available for sac spawners, which are often the numerically dominant copepods in estuarine and freshwater environments and therefore important in the diets of planktivorous fish (Kiørboe 1998). The dynamics of sac spawners, therefore, is critical to understanding trophic transfer within these ecosystems. However, our understanding of trophic dynamics in estuaries is largely location-specific, limiting the development of general paradigms on biological processes (Cloern and Jassby 2010).

Estuaries are frequently regarded as productive areas for pelagic species (Sheaves et al. 2014), and many are eutrophic (Nixon 1986). A recent global synthesis of primary productivity in estuaries, however, shows strong variability in phytoplankton production among regions, seasons, and years (Cloern

et al. 2014). Many estuaries are more accurately characterized as mesotrophic (100–300 g C m^{-2}yr^{-1}) or even oligotrophic (< 100 g C m^{-2} yr^{-1}), a category that includes the northern San Francisco Estuary (Cloern et al. 2014). Like many estuaries, the San Francisco Estuary is also degraded by human activities such as land modifications, contamination, overharvest, and introductions of non-native species, all of which may contribute to variability in primary production (Nichols et al. 1986; Cloern and Jassby 2010).

Low primary productivity in the nutrient-replete northern San Francisco Estuary (SFE) has been attributed to a combination of high turbidity and benthic grazing (Alpine and Cloern 1992). Primary productivity declined sharply in 1987 when the nonnative clam *Potamocorbula amurensis* became established in brackish to saline regions (Alpine and Cloern 1992; Cloern and Jassby 2012). Introductions of copepods and mysids have completely altered the zooplankton assemblages in this region and may have reduced foodweb efficiency which, together with reduced primary productivity, now limit the availability of food for declining pelagic fishes (Sommer et al. 2007; York et al. 2014). Understanding how copepod productivity responds to resource limitation is therefore essential for understanding the availability of copepods as nutrition for pelagic fishes in the SFE.

Two of the copepod species introduced to the SFE are of the sac-spawning, demersal genus *Pseudodiaptomus* (Walter 1987; Orsi and Walter 1991). *Pseudodiaptomus marinus*, first detected in the SFE in 1986, is a marine copepod first described in Japan that has spread throughout the northern hemisphere (e.g., Brylinski et al. 2012). *Pseudodiaptomus forbesi*, a brackish-water copepod originally from mainland Asia, was first detected in the SFE in 1987 and is abundant in brackish to freshwater regions of the SFE. Adults and copepodites of *P. forbesi* have a flexible pattern of vertical migration; in deep, turbid areas they migrate in synchrony with the tides resulting in retention (Kimmerer et al. 2002; 2014a), while in areas where light penetrates to the bottom they are demersal, remaining on the bottom by day (Kimmerer and Slaughter 2016). This species is omnivorous, consuming diatoms, flagellates, and ciliates (Bouley and Kimmerer 2006; Bowen et al. 2015; Kayfetz and Kimmerer 2017) as well as cyanobacteria including the toxic cyanobacterium *Microcystis aeruginosa* (Ger

et al. 2018; Holmes and Kimmerer *submitted*). Since its introduction, *P. forbesi* has been the most abundant calanoid copepod in the northern SFE (Orsi and Walter 1991; Kayfetz and Kimmerer 2017). After 1993, though, its distribution shifted eastward toward fresh water and it is now uncommon at salinities greater than 2 (Kayfetz and Kimmerer 2017), probably as a result of increased predation mortality to nauplii (Kayfetz and Kimmerer 2017; Kimmerer et al. 2019).

We synthesized data on growth rate and EPR of *P. forbesi* from published studies conducted during 2006–2016 with new data from 2017 and 2018. The objective of this synthesis was to investigate vital rates across a broader range of environmental conditions than had been encountered in any individual study. Each of the studies had different objectives and designs, but all collected data on chlorophyll *a* concentration (hereafter "Chl *a*") and in most cases both growth and egg production rates. We analyzed these data: 1) to broaden the data available to analyze the responses of *P. forbesi* copepodite growth and EPR to Chl *a* as a measure of productivity of the pelagic food web; 2) to determine if SEPR was useful as a proxy for copepodite growth in this species; and 3) to determine whether variation in vital rates among habitats of the northern SFE was due simply to variation in food supply as represented by Chl *a*, or to other characteristics of these habitats.

Materials and methods

Study area

The San Francisco Estuary includes (from west to east, i.e., seaward to landward) the open waters of San Francisco and San Pablo Bays, Carquinez Strait, and Suisun Bay, and the California Delta (Delta) formed by the confluence of the Sacramento and San Joaquin Rivers (Fig. 1). The Delta is a network of tidal sloughs and channels mostly confined between engineered levees that protect islands and mainland areas largely used for agriculture. Tidal flows vary across regions, from $\sim 12{,}000$ m^3 s^{-1} in Carquinez Strait, between 1800 and 5900 m^3 s^{-1} at the eastern end of Suisun Bay, to approximately 60 m^3 s^{-1} in the Cache Slough Complex of the northern Delta (Kimmerer 2004; Morgan-King and Schoellhamer 2013). Monthly mean freshwater flow from the Delta into Suisun Bay ("net

Delta outflow," hereafter "outflow") during 1980–2019 ranged from 50 to 7600 m^3 s^{-1}, with highest flows occurring during winter–spring (https://data.cnra.ca.gov/dataset/dayflow, accessed July 3, 2020).

In the northern Delta, the Yolo Bypass is a partially leveed floodplain built to protect the city of Sacramento from winter floods (Fig. 1). The Yolo Bypass has flooded in more than 60% of winters since its creation in the early 1930s, providing important spawning and rearing habitat for native fishes (Sommer et al. 2001). During the summer–autumn dry season, the Yolo Bypass is confined to a narrow (≤ 50 m wide) and shallow (≤ 5 m deep) tidal channel connected to the Cache Slough Complex (CSC) (Morgan-King and Schoellhamer 2013; Frantzich et al. 2018). The CSC is a tidal wetland comprising a network of turbid backwater channels and marshes that are rare elsewhere in the Delta (Whipple et al. 2012). During summer–autumn, water within the wetland and tidal channel is warmer, has longer residence times, and periodically has greater phytoplankton biomass than in adjacent open-water regions (Schemel et al. 2004; Gross et al. 2019).

We categorized our sampling and analyses into four habitat types: (1) brackish open water (salinity 0.5–6.8), which includes samples collected in Carquinez Strait, Suisun Bay and the tidal brackish reaches of the Sacramento and San Joaquin Rivers; (2) fresh open water (salinity < 0.5), which includes samples collected in Suisun Bay, and the tidal fresh Sacramento and San Joaquin Rivers; (3) the restored and remnant wetlands of the Cache Slough Complex (wetland); and (4) the perennial tidal channel (tidal channel) forming the eastern boundary of the Yolo Bypass floodplain (Fig. 1).

Field sampling and vital rate estimates

We collected samples during ten years from 2006 to 2018 from late spring to autumn (Tables 1, 2). Not all habitats were sampled in all years or months, and the wetland and tidal-channel habitats were sampled only in 2015–2018. We measured water temperature, salinity, turbidity, Secchi depth, and water depth, and collected site water for Chl *a* at each station (Fig. 2). Sometimes EPR and growth rate were measured on different days, and at other times only growth rate or EPR was measured (Table 2).
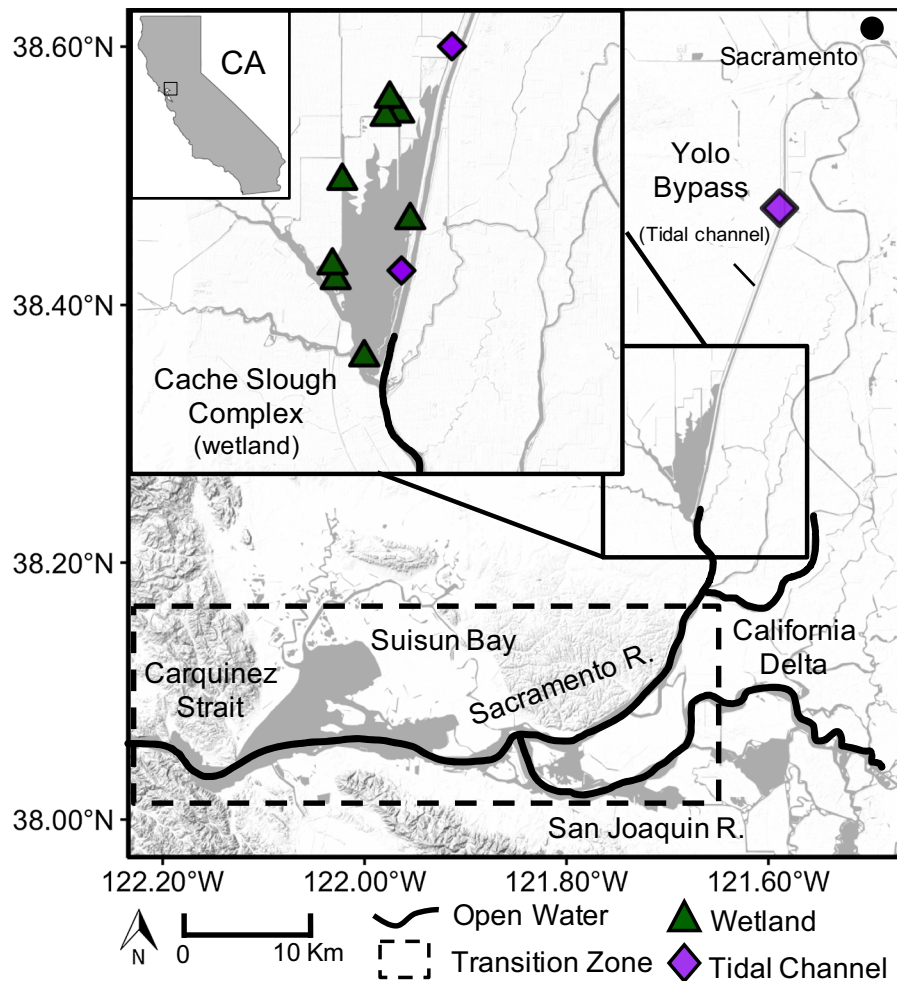
Fig. 1 Map of northern San Francisco Estuary, from Carquinez Strait to the northwestern California Delta. Sampling locations are identified by habitat type: open water (drawn line), wetland (filled triangle) and tidal channel (diamond). Dashed box indicates the estuarine transition zone of sampling where fresh and brackish open-water habitats converge (package *ggmap* in R, Kahle and Wickham 2013)

Temperature and salinity were measured using a Seabird SBE-19 CTD, handheld YSI Model 30, or handheld Hydrolab Sonde Quanta conductivity meter. Turbidity in some programs was measured with the Seabird SBE-19 or estimated from long-term monitoring data (see below) on turbidity (nephelometric turbidity units, NTU) and the inverse of Secchi depth (m) with a generalized linear model having an identity link and variance proportional to the mean squared [turbidity = $-1.27 + (1/\text{Secchi}) (7.93 \pm 0.05)$, $N = 12787$]. Surface water was collected in 2-L Nalgene polycarbonate bottles and immediately placed in a dark cooler containing wet ice for transport to the EOS Center (37.8895°N, 122.4470°W). At the laboratory,

usually within 3 h from water collection, we filtered three replicate samples of site water onto 25-mm-diameter GF/F filters (Whatman, nominal pore size 0.7 μm) and three onto 25-mm-diameter 5-μm polycarbonate filters (GE Water and Process Technologies). Filters were stored in the dark at -20 °C until analyzed. Pigments were extracted from the filters in 90% (v/v) acetone in the dark at -20 °C for 24 h, and fluorescence was measured with a Turner Designs 10-AU benchtop fluorometer calibrated annually with Chl *a* (Turner Designs) (Arar and Collins 1997). We report mean Chl *a* and mean Chl *a* > 5 μm of 3 filters of each type from one water sample collected at each site. During 2015–2016, we used Chl *a* data on GF/F

Table 1 Summary of *P. forbesi* growth-rate incubations ($N = 118$) conducted during 2006–2018

Years	Months	Habitat	Method	Incubation type
2006–2007[a]	May–Jul	Open water	AC mass	4-L Cubitainers® in outdoor water bath
2010–2012[b]	Aug–Oct	Open water	Molt rate	175-mL bottles, plankton wheel, constant-temperature room
2015[c]	Jun, Jul, Oct	Wetland	AC volume	4-L Cubitainers®, in situ moored floating raft
2015–2018[d]	Jul–Oct	Open water; tidal channel	AC volume	2015–2017: 4-L Cubitainers®, in situ moored floating raft;
				2018: 2-L bottles, plankton wheel, indoor water bath
2017–2018	Sep–Nov	Open water	AC volume	2017: 2-L bottles, plankton wheel, constant-temperature room;
				2018: 2-L bottles, plankton wheel, indoor water bath
2018	Aug, Sep	Wetland	AC volume	2-L bottles, plankton wheel, indoor water bath

Methods for measuring growth: artificial cohort (AC), using direct carbon measurements (mass, $N = 12$) or volume converted to carbon (volume, $N = 84$) using empirically derived volume-to-carbon calibration of copepodite life stages; molt rate ($N = 22$), using stage durations determined in the laboratory from field-collected copepods along with carbon mass by stage

[a]Kimmerer et al. 2014b

[b]Kimmerer et al. 2018b

[c]Kimmerer et al. 2018a

[d]Owens et al. 2019 (2015–2017 only)

filters only collected by the Department of Water Resources (DWR; Frantzich et al. 2018); samples taken in 2017–2018 by our laboratory were closely correlated with those taken by DWR at the same times and places (slope = 1.0, r = 0.97, 62 df).

During sampling in the tidal channel in 2017 and 2018, we also collected samples for analysis of lipid content of particulate matter as a measure of food quality. Details of methods are provided by Owens et al. (2019). Briefly, we filtered 800 mL (median; range 325–1500, depending on particulate concentration) whole-water samples onto pre-combusted 47-mm-diameter GF/F filters and shipped the frozen (− 80 °C) filters on dry ice to the Memorial University of Newfoundland Aquatic Research Cluster for analysis. Filters were ground in chloroform–methanol, and lipid classes were analyzed using Chromarod thin-layer chromatography with Iatroscan flame-ionization detection calibrated with standards for each lipid class from Sigma-Aldrich (Parrish 2013). Individual lipid compounds were identified and quantified using capillary gas chromatography with flame-ionization detection (Parrish 2013). Here, we use long-chain essential fatty acids (LCEFA), calculated as the sum of eicosapentaenoic acid (EPA), arachidonic acid (ARA), and docosahexaenoic acid (DHA), as a percentage of total fatty acids (Galloway and Winder 2015; Owens et al. 2019). The 2018 samples were delayed during shipment and reached room temperature for several days before analysis and were somewhat degraded (see Results).

We completed 118 growth-rate experiments with *P. forbesi* under conditions and using methods that varied among studies (Table 1). We examined residuals from the statistical models that best fit the data (see below) for evidence that these differences affected our interpretations but found none, though note that differences among habitats could be partly due to these differences in methods. Most growth-rate sub-samples were incubated in a constant-temperature room or water bath set to the ambient (i.e., site or collection) temperature. During 2015–2017 at the wetland and tidal-channel sites, incubation containers were placed in plastic netting suspended below a raft moored in an energetic tidal stream near the collection site (Kimmerer et al. 2018a; Owens et al. 2019).

In most of our studies (Table 1), we used a modified version of the artificial cohort (AC) method to estimate growth rates (Kimmerer and McKinnon 1987; Kimmerer et al. 2007). For the AC method, live copepods were collected by gentle sub-surface tows with a 150-μm mesh, 0.5-m-diameter ring net. We gently transferred copepods from the cod end of the net to a 20-L insulated cooler filled with 35-μm-filtered site water. The copepod assemblage was size-fractionated by gentle reverse filtration through nylon mesh filters

Table 2 Summary of methods and flow conditions for *P. forbesi* egg production rate (EPR) samples (*N* = 191)

Years	Months	Habitat	Timing	Net mesh size (μm)	Tow type	Net outflow (m³ s⁻¹)	
						Mean	Range
2006–2007[a]	May–Jul	Open water	Same date	53	Vertical	2006: 645	290–1000
						2007: 213	152–266
2010–2012[b]	Aug–Oct	Open water	∼ 2 d apart	53	Vertical	2010: 161	155–167
						2011: 313	251–346
						2012: 133	127–138
2016[c]	May, Jun	Open water; wetland	EPR only	53	Horizontal, 1 min	2016: 272	200–344
2015–2018	Jul–Oct	Open water; tidal channel	Same date	150	Horizontal, 3–5 min	2015: 132	127–137
						2016: 185	147–234
						2017: 453	273–796
						2018: 159	141–172
2017–2018	Sep–Nov	Open water	Same date	53	Vertical	2017: 296	256–366
						2018: 157	142–172
2018	Aug, Sep	Wetland	∼ 1 d apart	53	Horizontal, 1 min	2018: 163	163

"Timing" column indicates when EPR samples were taken in relation to growth-rate samples. All net tows with 0.5-m-diameter ring net; vertical tows to 10 m depth, or 1 m from bottom; horizontal tows just below water surface (max depth ∼ 0.5–1 m). Mean and range of outflow are for months in which sampling took place in each habitat (https://data.cnra.ca.gov/dataset/dayflow)

[a]Kimmerer et al. 2014b

[b]Kimmerer et al. 2018b

[c]Jungbluth et al. 2020

to obtain the size range 200–224 μm, approximately the size expected for C1–C3 *P. forbesi* copepodites. Subsamples from this artificial cohort were taken to obtain ∼ 30–40 copepods L⁻¹ and transferred alternately to incubation containers and to jars for preservation. Containers were either 2-L square PETG Nalgene bottles or 4-L Cubitainers® filled with 35-μm-filtered surface water from the site. Samples in containers were incubated for 1–4 days depending on temperature. Initial and incubated samples were preserved in 2% (final conc.) glutaraldehyde which minimizes change in mass or volume during preservation (Kimmerer and McKinnon 1986).

Copepod carbon for calculating growth rates was measured in one of two ways—directly and from volumes of individual copepods. In 2006–2007, all copepods from each growth-rate subsample were dried and analyzed for particulate carbon with an elemental analyzer (method called "AC mass," Table 1; Kimmerer et al. 2014b). Thereafter, we used image analysis (Alcaraz et al. 2003) to estimate volume of each copepod which was calibrated to carbon. Aliquots of preserved samples were examined, and

all *P. forbesi* were transferred to a Petri dish, and this process was repeated to obtain a total of at least 30 copepods. Copepods were measured using a Spot Idea S8APO digital camera mounted to a Leica M125 dissecting microscope, and ImageJ software was used to estimate volume (mm³) of each copepod, which was converted to carbon mass ("AC volume," Table 1) using an empirical volume/carbon calibration for *P. forbesi* with a prediction error of 14% (Kimmerer et al. 2018a; Owens et al. 2019). For both AC mass and AC volume, growth rate was calculated as the slope of ln (carbon) versus time of incubation with a linear model over the entire incubation period. In 93 growth-rate measurements, we terminated some replicate incubation samples at intermediate time points as a check on linearity. These were analyzed using a linear model with an additional parameter for a change in slope after the first incubation interval. In nine of these 93 measurements, growth rates changed during the incubation period, so for these growth rate was determined only over the first incubation interval (1 or 2 d).

During 2010–2012, we used the modified molt-rate method to determine growth rates (Hirst et al. 2014;
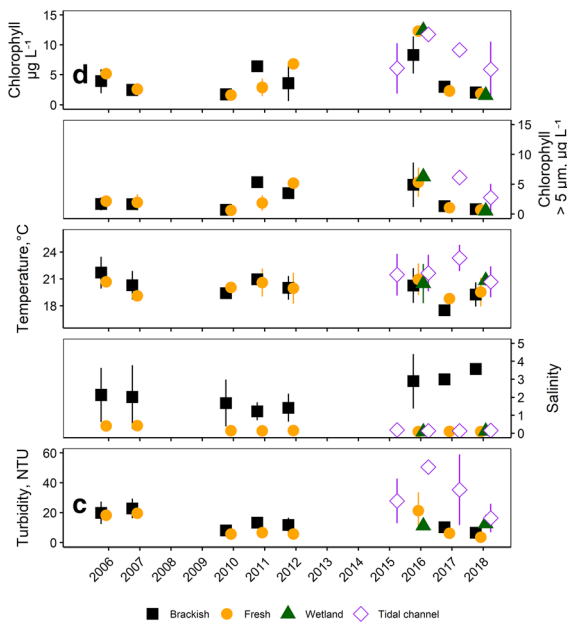
Fig. 2 Environmental conditions by habitat (symbols) in SFE during sampling for growth rate and egg production estimates, 2006–2018. Each data point gives the mean and 95% confidence intervals around the mean for all samples taken during each year; some confidence intervals fall within the height of the symbol. Points have been moved slightly in the x direction to make all points visible: **a** concentration of chlorophyll *a* collected on GF/F filters and **b** on 5-μm filters; **c** temperature; **d** salinity (Practical Salinity Scale); **e** turbidity

Kimmerer et al. 2018b). Live copepods were collected and handled as for the AC method. In the laboratory, we pipetted individual copepods into 175-mL bottles filled with 35-μm-filtered site water. Bottles were placed on a plankton wheel rotating at 1 rpm in a constant-temperature room for 48 h. At the end of each incubation, bottles were filtered onto a 35-μm mesh screen and copepods were transferred to 20-mL glass vials, stained with Chlorazol Black E, and preserved with 4% (final conc.) formaldehyde. Preserved samples were later examined for the presence of a stained copepod and at least one exuvia. A development-rate index was estimated as the ratio of the fraction of copepods that molted to the expected fraction from laboratory experiments, adjusted to field temperatures. Growth rate was calculated as the product of laboratory-determined growth rate adjusted to field temperature and this development-rate index. To account for the uncertainties in laboratory growth and development and count data, we calculated the

development-rate index and growth rate using Bayesian hierarchical models (Kimmerer et al. 2018b).

We estimated 191 EPRs of *P. forbesi*. Live copepods were collected with 0.5-m-diameter plankton nets with some variation in mesh sizes and methods (Table 2). Cod-end contents were immediately transferred to sample jars and preserved in 4% (final conc.) buffered formaldehyde. Egg production rates were estimated using the egg-ratio method (Edmondson et al. 1962) with egg development time calculated from ambient (i.e., site or collection) temperature using an equation in Sullivan and Kimmerer (2013). In the laboratory, one or more representative subsamples were taken and all adult *P. forbesi* females were identified as either ovigerous or non-ovigerous. Egg sacs attached to females were removed and eggs counted from at least 30 ovigerous females, or all females in the subsample, and loose egg sacs identified as those of *P. forbesi* were dissected and their eggs were counted. The mean number of eggs per sac in the sample was used to extrapolate to any additional ovigerous females in the subsample. The egg ratio was calculated by dividing the sum of all eggs by the sum of all females in the subsample (or sample). Data used here were restricted to samples with at least 20 total females (median 126, maximum 838) to minimize the effect of high relative error in low counts.

Most of our field sampling for growth rate and EPR occurred at the same location and time, but because of logistical constraints some samples for growth rate and EPR were collected on different dates and somewhat different locations (Table 2). In 2010–2012, EPR samples were collected ~ 2 d before or after growth-rate incubations were initiated and we linked growth rate to mean egg production rates from three or four EPR stations near the growth-rate collection sites (Table 2; Table 1 in Kimmerer et al. 2018b). In 2018, we initiated growth-rate incubations 1 d before EPR samples were collected at the same locations. For these samples, we linked growth and EPRs as if they had been collected on the same day and location to allow for comparison with our other studies.

Specific egg production rate (SEPR) was calculated using EPR and the ratio of egg carbon to female carbon (Kimmerer et al. 2014b, 2018b). We used reported summertime female carbon content (4 μg C per female, Kimmerer et al. 2018b) and calculated mean

egg carbon content from mean egg diameter (97 μm, Kimmerer et al. 2014b) and a carbon/volume ratio of 0.13 pg C μm^{-3} (Kiørboe and Sabatini 1995; Uye and Sano 1995), so that SEPR = EPR × 0.015. Female size can be inversely related to temperature (McLaren 1965), but we did not determine female size for all adult copepods in our analyses. The inter-quartile range of temperature for all samples used in our analyses was ≤ 9 °C, and we expect any error associated with using mean female size to calculate SEPR to be small.

Long-term monitoring data

We obtained zooplankton abundance data from a long-term monitoring program to provide context for our vital rate estimates. The California Interagency Ecological Program (IEP) has maintained a zooplankton monitoring program since 1972, collecting monthly samples throughout larger channels in the northern SFE (Environmental Monitoring Program, Orsi and Mecum 1986; Winder and Jassby 2011). To ensure the wetland habitat was represented, we also obtained *P. forbesi* abundance data from the spring 20-mm fish-monitoring program run by California Fish and Wildlife (CDFW) for IEP (Dege and Brown 2004). Complete data sets are available from CDFW (https://portal.edirepository.org/nis/mapbrowse?scope=edi&identifier=539 accessed January 17, 2021), and methods are outlined in the Supplement. Adult *Pseudodiaptomus* in these samples were identified to species, and copepodites to genus; since *P. marinus* adults were rare in all of our samples, we assumed all copepodites were *P. forbesi*. Neither of these monitoring programs collected samples in the tidal channel so we used our own copepod abundance data from 2015 to 2018. Previous studies have demonstrated similar abundance patterns between the IEP monitoring program and our sampling (Kimmerer et al. 2014b, 2018a).

After merging the monitoring data sets, we calculated mean abundance by year and habitat for late spring–autumn (May–Oct). The abundance data had a roughly log-normal distribution with some zeros, so we calculated geometric means after adding 10 to each value.

Statistical analyses

The analyses in this study were necessarily limited by the use of data from different studies collected for different purposes and in different locations, years, and months. Formal statistical tests are unwarranted for this data set, especially given the trend in the scientific literature away from formal testing and toward fitting models and estimating their parameters (e.g., Wasserstein and Lazar 2016; Smith 2020). Therefore, we developed statistical models and estimated their parameters, being mindful of the incomplete design of the data set. Our default approach was to use all the data available and to examine the effects of alternative models graphically and with statistics including the Akaike information criterion (AIC, Akaike 1974). Model fits were examined using standard diagnostic procedures such as normal probability plots. Analysis and model fitting were done in R version 4.2 (R Core Team 2020). Functions used included *lm* and *nls* for linear and nonlinear models, *glm* for generalized linear models, *ggplot2* v. 3.3.2 (Wickham 2016) and *patchwork* v. 1.1.1 (Pederson 2020) for graphics, and *predictNLS* (*propagate* package v. 1.0–6, Spiess 2018) for predicting output from *nls* with error bands. Parameters for all fitted models are listed in Table 3.

A linear model was used to determine the relationship between the log of growth rate of *P. forbesi* and ambient temperature. To allow for comparison of growth rates conducted at different temperatures, we adjusted to a common temperature of 22 °C using the exponential fit for egg development time to temperature from Sullivan and Kimmerer (2013). This temperature was used in a laboratory estimate of maximum growth rate (Kimmerer et al 2018b) and is typical of the study area during summer. Temperature-adjusted growth rates were related to SEPR using a geometric mean regression (Ricker 1973), suitable when both variables are determined with substantial error. Error terms presented throughout the text and figures refer to 95% confidence intervals of the mean unless stated otherwise.

Laboratory experiments measuring growth of *Calanus pacificus* and *Pseudocalanus* spp. by Vidal (1980) and EPR of *Paracalanus parvus* by Checkley (1980) showed saturating hyperbolic responses to food concentration. We determined the relationships of *P. forbesi* copepodite growth rate and SEPR to Chl *a* by

fitting data to a rectangular hyperbola identical to a type II functional response for feeding:

$$g = C(g_{max})/(C + K_g) \qquad (1)$$

$$E = C(E_{max})/(C + K_e) \qquad (2)$$

where g is growth rate (d^{-1}), E is EPR (eggs $\female^{-1}\,d^{-1}$), g_{max} and E_{max} are maximum growth rate and EPR, respectively, C is Chl a ($\mu g\,L^{-1}$), and K_g and K_e are the half-saturation constants of growth and EPR, respectively. An alternative set of models was fitted in which the maxima could vary among habitats:

$$g = C\ (g_{max}[h])/\ (C + K_g) \qquad (3)$$

$$E = C(E_{max}[h])/(C + K_e) \qquad (4)$$

where $g_{max}[h]$ and $E_{max}[h]$ are the maxima for each coefficient that vary among the four habitats h. Alternative models were also tried in which the K values or both parameters were allowed to vary with habitat, but they fit the data no better than the models in Eqns. 1–4.

These models assume that Chl a was measured with relative errors smaller than those of the response variables. We took analytical replicates, but because of time constraints we did not take true replicates for Chl a. We obtained a measure of uncertainty in Chl a concentration using continuous in situ monitoring data from several stations near our sampling locations (Jungbluth et al. 2020) and estimated a coefficient of variation of $\sim$ 10% using those data (see Supplement). This is small compared to the variation in growth or egg production rates, so we ignored it for fitting but used it in displaying model predictions.

We compared the fits of Eqs. 1 and 2 with those from three alternative models with the same data: a nonlinear model identical to those in Eqs. 1 and 2 but with an intercept term, a linear model with no intercept under the assumption that growth was zero when food concentration was zero, and a constant model. Using AIC, we found that the hyperbolic models without intercept were superior to the alternatives for both growth rate and EPR (not shown). This also satisfied our expectation that growth rate and SEPR should be near zero when Chl a was zero and reach a plateau at high Chl a. To assess the effect of habitat, we fit alternative models in Eqs. 3 and 4 and compared them with corresponding simpler models using AIC and other diagnostics. Finally, residuals from the best-fitting models (Eqs. 1–4) were plotted against the remaining environmental variables to determine if they contributed to variation in growth or EPR.

During 2017 and 2018 in the tidal channel, growth and egg production rates were analyzed for responses to the percent of LCEFA in fatty acids using rectangular hyperbolas as in Eqs. 1 and 2 with LCEFA % substituted for Chl a (Owens et al. 2019). To account for thermal degradation of samples taken in 2018, we included year as a covariate, but comparison of models with and without year using AIC showed that year did not improve the fit. Moreover, an analysis of covariance of LCEFA % with Chl a as predictor and year as a factor revealed that predicted LCEFA % was lower by $1.4 \pm 1.3\%$ in 2018 than in 2017, further suggesting that the effect of degradation on these results was minor.

Results

Mean annual freshwater flow into the San Francisco Estuary (net outflow) by water year (November–October) ranged from 169 to 1940 $m^3\,s^{-1}$. The years 2006, 2011, and 2017 were wet ($> 1000\ m^3\,s^{-1}$), but summer flows were generally low (Table 2). Environmental conditions varied by year and among habitats (Fig. 2). In 2016 a widespread bloom of the diatom *Aulacoseira* sp. elevated Chl a in all freshwater areas and to some extent in brackish water (Fig. 2a, b). In other years, the highest Chl a values were mostly in the tidal channel while the open-water areas generally had Chl $a < 5\ \mu g\,L^{-1}$. Chlorophyll larger than 5 μm comprised half of total Chl a on average, and this fraction did not differ among habitats when they were sampled in the same year (Fig. S1a). Total Chl a was linearly related to Chl $a > 5\ \mu m$ with a slope of 1.14 ± 0.09 and an intercept of $1.6 \pm 0.5\ \mu g$ Chl $a\,L^{-1}$ (Fig. S1b, Table 3). Temperature was not highly variable among habitats or years (Fig. 2c), and salinity was above 1 only in the brackish habitat (Fig. 2d). Median turbidity was highest in the tidal channel, and brackish open water was usually more turbid than fresh open water (Fig. 2e).

Interannual patterns of abundance of *P. forbesi* copepodites and adults were similar in all habitats studied except in the tidal channel (Fig. 3). *Pseudodiaptomus forbesi* was more abundant in fresh open water than in brackish open water, except in wet years 2006, 2011, and 2017 (Fig. 3a, b). Copepodites were

Table 3 Parameters of best statistical models for growth (g) and egg production rate (EPR)

Response	Figure	Model	Predictors	Coefficients	Residual SE	Variance explained	N
Growth	4	Log-linear	Temperature	$Ln(g) = -3.8 + (0.105 \pm 0.034)\ T$	0.45	25%	115
Growth at 22 °C	5	Eq. 1	Chl	$g_{max} = 0.37 \pm 0.055$ $K_g = 1.6\ (0.9, 2.6)$	0.09	24%	118
	5	Eq. 3	Chl, habitat	$g_{maxB} = 0.32 \pm 0.08$ $g_{maxF} = 0.28 \pm 0.07$ $g_{maxW} = 0.38 \pm 0.09$ $g_{maxT} = 0.35 \pm 0.02$ $K_g = 1.1\ (0.5, 2.0)$	0.09	29%	118
	8a	Eq. 1	Chl > 5 μm	$g_{max} = 0.24 \pm 0.035$ $K_g = 0.1\ (0, 0.3)$	0.09	3%	118
	Not shown	Eq. 3	Chl > 5 μm, habitat	$g_{maxB} = 0.25 \pm 0.05$ $g_{maxF} = 0.21 \pm 0.04$ $g_{maxW} = 0.31 \pm 0.07$ $g_{maxT} = 0.25 \pm 0.04$ $K_g = 0.1\ (0, 0.3)$	0.09	13%	118
Growth at 15 °C	–	Eq. 1	Chl	$g_{max} = 0.16 \pm 0.02$ $K_g = 1.6\ (0.9, 2.6)$	0.04	24%	118
Growth residual	S4	Linear	Salinity	Slope $= -0.002 \pm 0.02$	–	–	118
			Secchi, cm	Slope $= -0.0002 \pm 0.0003$	–	–	84
			Depth, m	Slope $= -0.002 \pm 0.005$	–	–	68
			Turbidity, NTU	Slope $= 0.001 \pm 0.001$	0.1	2%	94
Egg production	7	Eq. 2	Chl	$E_{max} = 4.1 \pm 0.5$ $K_e = 3.9\ (2.1, 6.6)$	1.5	19%	191
	7	Eq. 4	Chl, habitat	$E_{maxB} = 3.3 \pm 1.1$ $E_{maxF} = 3.5 \pm 1.0$ $E_{maxW} = 8.0 \pm 2.1$ $E_{maxT} = 3.6 \pm 0.9$ $K_e = 2.9\ (1.5, 5.0)$	1.4	28%	191
	Not shown	Eq. 2	Chl > 5 μm	$E_{max} = 3.2 \pm 0.9$ $K_e = 1.1\ (0.4, 2.1)$	1.6	11%	168
	8b	Eq. 4	Chl > 5 μm, habitat	$E_{maxB} = 2.6 \pm 0.8$ $E_{maxF} = 2.7 \pm 0.7$ $E_{maxW} = 7.2 \pm 1.9$ $E_{maxT} = 2.8 \pm 1.0$ $K_e = 0.7\ (0.3, 1.4)$	1.5	24%	168
Egg production residual	S5	Linear	Salinity	Slope $= -0.003 \pm 0.02$	–	–	191
			Secchi, cm	Slope $= -0.00006 \pm 0.003$	–	–	167
			Depth, m	Slope $= -0.01 \pm 0.06$	–	–	137
			Turbidity, NTU	Slope $= 0.005 \pm 0.01$	–	–	185
Growth	9	Geometric mean	SEPR	Slope $= 5.2 \pm 1.3$ Intercept $= 0.09 \pm 0.03$	–	$R = 0.29$	92

Table 3 continued

Response	Figure	Model	Predictors	Coefficients	Residual SE	Variance explained	N
Growth at 22 °C vs. lipids and chlorophyll	10a	Eq. 1 mod	LCEFA%	$g_{max} = 0.37 \pm 0.26$ $K_g = 4.2\ (0.4, 16)$	0.08	16%	34
	10b	Eq. 1	Chl	$g_{max} = 0.29 \pm 0.07$ $K_g = 1.0\ (0.2, 2.4)$	0.08	20%	34
Egg production vs. lipids and chlorophyll	10c	Eq. 2	LCEFA%	No fit	–	–	31
	10d	Eq. 2	Chl	$E_{max} = 7\ (3, 93)$ $K_e = 14\ (4, 338)$	1.6	32%	31
Chlorophyll size	–	Linear model	Habitat	Brackish $= 0.58 \pm 0.06$ Fresh $= 0.54 \pm 0.05$ Wetland $= 0.50 \pm 0.14$ Tidal $= 0.51 \pm 0.09$	0.28	NA	251
	S1b	Linear model	Chl $> 5\ \mu$m	Slope $= 1.14 \pm 0.09$ Intercept $= 1.6 \pm 0.5$	2.9	0.75	214

Coefficients are given with confidence intervals, in parentheses if asymmetrical. Subscripts for coefficients are first letters of habitats: brackish open water, fresh open water, wetland, and tidal channel

generally more abundant in the wetland and tidal channel than in the brackish and fresh open waters (Fig. 3). In the tidal channel, sampled only from 2015 to 2018, copepodite abundance averaged ~ 35-fold higher than adult abundance (Fig. 3d).

Pseudodiaptomus forbesi growth rates averaged $0.21 \pm 0.05\ d^{-1}$ across all sampling events and habitats (Table 4) and were positively related to temperature with a slope similar to that used to adjust growth rates to a common temperature of 22 °C (Fig. 4; see Table 3 for parameters of all fitted relationships). Unadjusted growth rates did not differ between the brackish and fresh open-water habitats when both were sampled, but were generally higher in the wetland and tidal-channel habitats than in the open-water habitats (Fig. S2a). Seasonal patterns in growth rate were not strong, though there was a general decline toward the end of the year, mainly a response to temperature (Fig. S3a). The model for growth rate adjusted to 22 °C as a function of whole Chl a (Eq. 1, Fig. 5, thin lines, Table 3) explained 24% of the variance. One value from the wetland and one from the tidal channel exceeded the laboratory-derived maximum growth rate ($\sim 0.51\ d^{-1}$). Equation 3 (Fig. 5 thick lines, Table 3) fit slightly better than Eq. 1 (AIC difference of 3), but that difference was influenced by the single high growth rate in the wetland and the single high Chl a in the fresh open-water site; without those two data points the difference

in AIC was negligible at 0.8. Because of the high influence of the two data points, the unavoidable covariance between K_g and g_{max}, and the limited overlap among sample periods for habitats, we used the simpler model (Eq. 1) to represent the relationship of growth rate to Chl a. Residuals from Eq. 1 had no apparent relationship to environmental variables (Table 3, Fig. S4).

Pseudodiaptomus forbesi egg ratios (eggs $\female^{-1}$) showed no relationship to temperature (Fig. 6). Egg production rate averaged 2.0 eggs $\female^{-1}\ d^{-1}$ across all sampling events and habitats and reached a maximum of 11 eggs $\female^{-1}\ d^{-1}$ (Table 5). Egg production rates had no apparent trend over years and were similar among habitats when more than one was sampled (Fig S2b); a downward trend through the seasons was mainly due to changes in temperature (Fig. S3b). A rectangular hyperbola between EPR and Chl a (Eq. 2) explained only 19% of the variance in EPR, which was improved by adding habitat as a covariate (Eq. 4, Fig. 7, Table 3). The habitat effect was largely due to the elevated EPR in the wetland (Fig. 7c), which was based on only seven data points from two years (Table 2). Residuals from Eq. 4 had no apparent relationship to environmental variables (Table 3, Fig. S5).

Using Chl $a > 5\ \mu$m as a predictor in place of whole Chl a did not improve the fits either for growth rate adjusted to 22 °C or EPR (Fig. 8, Table 3). The fit
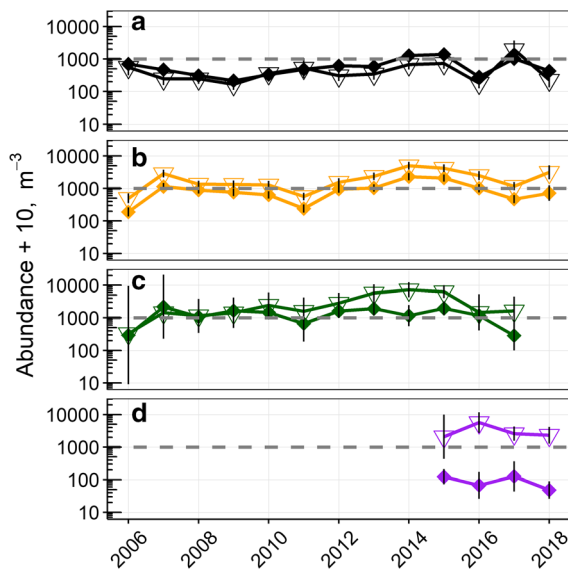
Fig. 3 *Pseudodiaptomus forbesi* abundance in SFE during late spring–autumn (year days 120–304), 2006–2018. Adults are filled diamonds; copepodites are inverted triangles. Abundance values are plotted as volumetric means plus 10 with error bars representing 95% confidence intervals. The y-axes are logarithmic scale. Abundance data from IEP long-term zooplankton monitoring program (**a** brackish open water; **b** fresh open water), CDFW spring 20-mm fish survey (**c** wetland), and Owens et al. (2019) (2015–2017) (**d** tidal channel). Horizontal dashed line drawn at 1000 m^{-3} to compare habitats

for growth rate was exceptionally poor, explaining only $\sim$ 3% of the variance using Eq. 1 and 13% using Eq. 3 (Table 3). The fits for EPR using Chl a > 5 μm were better than those for growth whether using Eqs. 2 or 4 (Table 3), but still explained less of the variance than did either Eqs. 2 or 4 using whole Chl a. Regardless of the equation, the half-saturation constants K_g and K_e were much lower for Chl a > 5 μm than for whole Chl a (Table 3).

All estimates of SEPR were well below the laboratory-derived maximum copepodite growth rate of $\sim$ 0.51 d^{-1}, and SEPR was lower than growth rate when compared pairwise except for one pair in which growth rate was negative with large error bars (Fig. 9). Growth rate and SEPR were weakly correlated and a geometric mean regression of growth rate on SEPR gave a slope of 5.2 and an intercept of 0.09 d^{-1} (Fig. 9, Table 3). Thus, SEPR was positively related to growth rate, but the intercept implied copepods grew at 0.09 d^{-1} even when SEPR was zero (Fig. 9).

Growth rates determined in the tidal channel and adjusted to 22 °C had a similar response to LCEFA %

as to Chl a when both were determined (2017 and 2018; Fig. 10a, b, Table 3), and had nearly identical residual standard errors of 0.08 d^{-1}. A similar model for egg production rate showed a weak response for Chl a and no response for LCEFA % (Fig. 10c, d). Parameter estimates for Chl a in this subset (Table 3) were consistent with those from the entire data set (Figs. 5, 7) though with wider confidence intervals reflecting the smaller sample size. Adding year as a covariate to the nonlinear models for LCEFA % did not improve the fits, as determined by AIC.

Discussion

Results from the two earliest studies included in this paper (Tables 1, 2) showed little to no relationship between the vital rates of *Pseudodiaptomus forbesi* and Chl a in the SFE, partly because of the limited range of Chl a in those studies (Kimmerer et al. 2014b, 2018b). By combining the results of studies in a variety of habitats and at times of elevated Chl a, this study has clarified these relationships.

Using all of the available data, the growth rate of *P. forbesi* was described by a hyperbolic function of Chl a (Fig. 5). Although growth rate was strongly associated with habitat—chronically low in the open water and sometimes high in the wetland and tidal channel (Fig. 5)—nearly all of this spatial variability was related to differences in Chl a, and only a few data points hinted at differences among habitats not explained by Chl a. Moreover, effects of other covariates were negligible. Chl a predicted EPR nearly as well as it did growth rate, and the fit was strengthened with habitat as a covariate (Fig. 7). Below, we compare Chl a with other proxies for copepod food, the role of reproductive strategy in copepod vital rates, and the differences in vital rates between copepodites and adult females and how those rates respond to the environment. Last, we explore the physical and biological processes controlling estuarine primary productivity and how this variability affects consumers such as copepods and pelagic fish.

Proxies for copepod food quantity and quality

Chlorophyll a concentration is the most widely used proxy for food available to copepods (Hirst and Bunker 2003; Bunker and Hirst 2004). It can be

Table 4 *Pseudodiaptomus forbesi* copepodite growth rates in SFE

Years	Months	Habitat	Observed growth rate Mean ± CI	Adjusted growth rate 22 °C				
				SD (N)	Range	Mean ± CI	SD (N)	Range
2006–2007[a]	May–Jul	Open water	0.14 ± 0.04	0.07 (12)	− 0.01–0.24	0.16 ± 0.05	0.08 (12)	− 0.01–0.28
2010–2012[b]	Aug–Oct	Open water	0.18 ± 0.02	0.04 (22)	0.09–0.24	0.23 ± 0.03	0.06 (22)	0.09–0.32
2015[c]	Jun, Jul, Oct	Wetland	0.35 ± 0.09	0.10 (9)	0.23–0.53	0.30 ± 0.13	0.20 (9)	0.15–0.68
2015– 2018[d]	Jul–Oct	Open water; tidal channel	0.27 ± 0.03	0.10 (56)	0.03–0.47	0.27 ± 0.03	0.10 (56)	0.03–0.54
2017–2018	Sep–Nov	Open water	0.12 ± 0.03	0.06 (15)	0.06–0.27	0.18 ± 0.05	0.09 (15)	0.09–0.42
2018	Aug, Sep	Wetland	0.19 ± 0.10	0.06 (4)	0.11–0.25	0.21 ± 0.11	0.07 (4)	0.12–0.28
All			0.21 ± 0.05	0.07 (118)	− 0.01–0.53	0.22 ± 0.07	0.10 (118)	− 0.01–0.68

Means with 95% confidence intervals (CI), standard deviations (SD) and number of experiments (N); ranges are the lowest and highest values. Last row ("All") reports statistics across all sampling events, 2006–2018

[a]Kimmerer et al. 2014b

[b]Kimmerer et al. 2018b

[c]Kimmerer et al. 2018a

[d]Owens et al. 2019 (2015–2017 only)
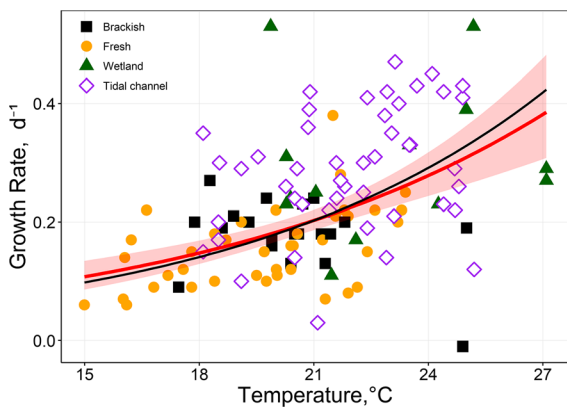
Fig. 4 *Pseudodiaptomus forbesi* copepodite growth rate (d^{-1}) as a function of *in situ* temperature. Red line is a linear regression (parameters in Table 3), and shading is 95% confidence interval for the model's prediction. Black line is the relationship of the inverse of egg development time to temperature (Sullivan and Kimmerer 2013) adjusted to cross the red line at the median temperature

measured cheaply and rapidly, it is correlated with phytoplankton primary production (Cole and Cloern 1987) and thereby energy supply to the pelagic food web (Sobczak et al. 2005), and it is frequently measured in studies of copepod ecology and energy flow, allowing comparisons among studies (Hirst and Bunker 2003).

The limitations of Chl *a* as a proxy for food of copepods are apparent in the high variability around the functions fitting both growth rate and egg production rate to Chl *a* (Figs. 5, 7, and 8). However, there are both statistical and ecological reasons why predictability is poor for these field-based measurements. Statistical impediments to a tight fit include the preponderance of the data at low Chl *a* concentrations (median 3 μg Chl *a* L^{-1}) which limits resolution of both parameters, and the uncertainty in Chl *a* measurements (coefficient of variation $\sim$ 10%) which induced some uncertainty in the half-saturation parameters (Figs. 5, 8, Table 3). In addition, growth rates were measured with a mean coefficient of variation of 14% of individual measurements and some highly uncertain values (error bars in Fig. 5). Finally, the variance–covariance matrix from the fits of Eqs. 1–4 showed that half-saturation constants were positively correlated with the maximum rates, which inflates the uncertainty in each parameter. For example, $r = 0.87$ between g_{max} and K_g for data in Fig. 5 (correlation not shown). Although the values of these correlations are not of particular interest, the correlations inflate the uncertainty of both model parameters. This problem of fitting asymptotic curves is unavoidable but has been largely ignored in the literature on feeding, growth, and EPR.
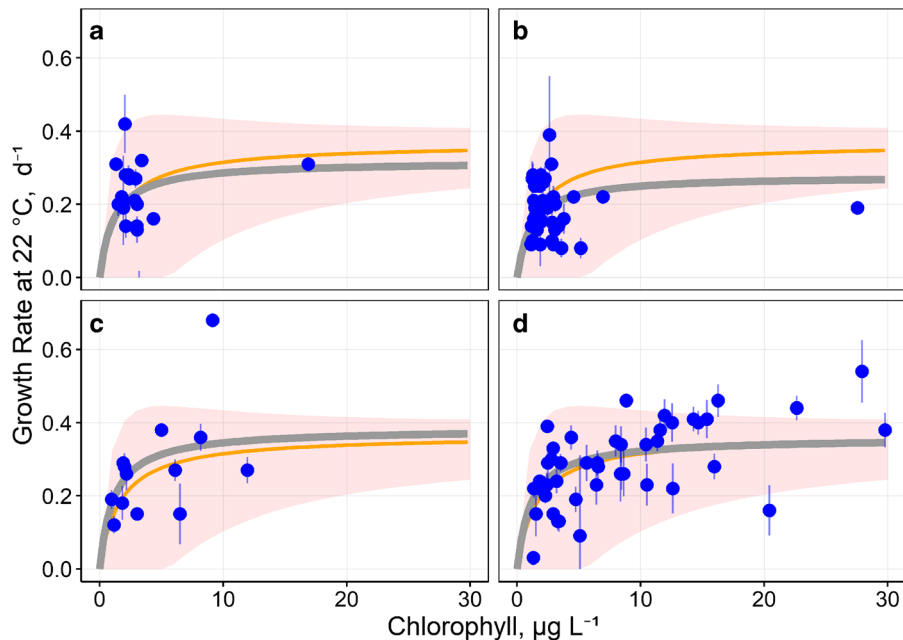
Fig. 5 *Pseudodiaptomus forbesi* copepodite growth rate (d^{-1}) adjusted to 22 °C, as a function of whole Chl *a* for each habitat in SFE: **a** brackish open water; **b** fresh open water; **c** wetland; **d** tidal channel. Lines are rectangular hyperbolas: the thin line was fitted to all data using Eq. 1, and the thick line was fitted with g_{max} allowed to vary among habitats (Eq. 3). Shaded area, 95% confidence interval for the model in Eq. 1, assuming that Chl *a* is estimated with an error having a standard deviation on the log scale of 0.1. Parameter values in Table 3
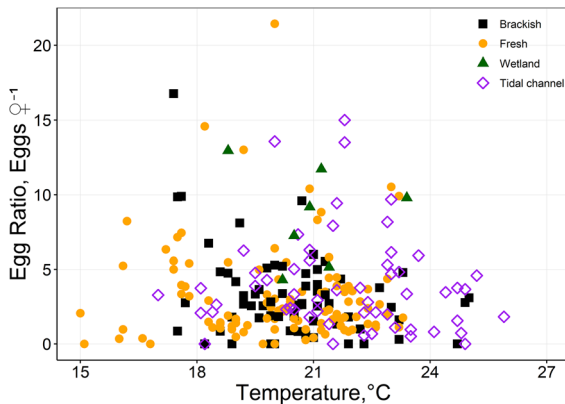
Fig. 6 *Pseudodiaptomus forbesi* female egg ratios in SFE (2006–2018) as a function of temperature at the collection site

The predictive capacity of Chl *a* is also subject to numerous ecological constraints. First, Chl *a* is a rather crude proxy for phytoplankton biomass, as the ratio of Chl *a* to phytoplankton carbon concentrations can vary with phytoplankton species, cell sizes, growth rates, and light levels (Eppley and Sloan 1966; Kiørboe 1993). During the 2006–2007 study (Table 1), the median ratio of organic carbon estimated from counts and measurements of phytoplankton cells and Chl *a* in 2007 was about double that in 2006, and organic carbon was more closely related than Chl *a* to primary productivity measured by incubation with ^{14}C (Kimmerer et al. 2012; Parker et al. 2012).

Second, copepods generally capture particles larger than $\sim$ 5–20 μm more efficiently than smaller particles (Hirst and Bunker 2003). However, the poor fits of the models using Chl *a* > 5 μm (Fig. 8), and the low half-saturation constants relative to uncertainty in Chl *a* measurements, suggest that these curves do not reflect a growth response to a particular food size class. Like other copepods (Stoecker and Egloff 1987; Saiz and Calbet 2011), *P. forbesi* readily consumes microzooplankton (Bouley and Kimmerer 2006; Bowen et al. 2015; Kayfetz and Kimmerer 2017). Thus, the fits in Figs. 5, 7, and 8 may indicate that Chl *a* is more a measure of energy supply to the pelagic food web which includes both large and small cells, supporting the copepods directly and through the unobserved microzooplankton.

Table 5 *Pseudodiaptomus forbesi* female egg production rate (EPR) in SFE by individual study

Years	Months	Habitat	EPR (Eggs ♀⁻¹ d⁻¹)		
			Mean ± CI	SD (N)	Range
2006–2007[a]	May–Jul	Open water	1.5 ± 0.6	1.0 (15)	0.0–3.2
2010–2012[b]	Aug–Oct	Open water	1.5 ± 0.2	0.8 (84)	0.1–3.7
2016[c]	May, Jun	Open water	4.2 ± 1.2	2.5 (20)	0.8–10.6
2015–2018	Jul–Oct	Open water; tidal channel	2.1 ± 0.5	1.7 (56)	0.0–8.3
2017–2018	Sep–Nov	Open water	1.1 ± 0.6	0.9 (12)	0.1–2.7
2018	Aug–Sep	Wetland	3.9 ± 3.1	2.0 (4)	2.2–6.7
All (2006–2018)			2.0 ± 0.2	1.6 (191)	0–10.6

Means with 95% confidence intervals (CI), standard deviations (SD), and number of estimates (N); ranges are the lowest and highest values. Last row ("All") reports mean EPR, CI, and SD, and N across all sampling events

[a]Kimmerer et al. 2014b

[b]Kimmerer et al. 2018b

[c]Jungbluth et al. 2020
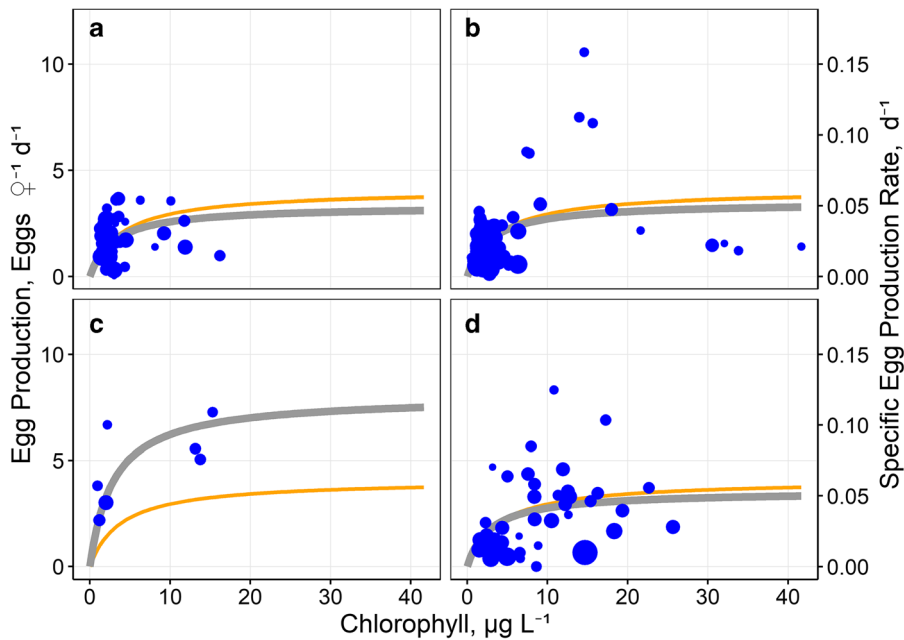
Fig. 7 *Pseudodiaptomus forbesi* female egg production rate (EPR, left axis) and specific egg production rate (SEPR, right axis) as a function of whole Chl *a* by habitat: **a** brackish open water; **b** fresh open water; **c** wetland; **d** tidal channel. Lines are rectangular hyperbolas: the thick line was fitted to all data using Eq. 2, and the thin line was fitted with g_{max} allowed to vary among habitats (Eq. 4). Parameters in Table 3

Third, samples for Chl *a* are taken at time and space scales that diverge widely from those governing the vital rates of copepods. For example, we collected zooplankton at a spatial scale of cubic meters and phytoplankton at a scale of liters, introducing spatial uncertainty into estimates of the food environment actually encountered by the copepods. A temporal disconnect between measures of food and vital rates arises both from the time interval between sampling for growth rate and for Chl a in two of our studies (Table 2), and from the time needed to convert food to copepod biomass. For example, female *Acartia tonsa*
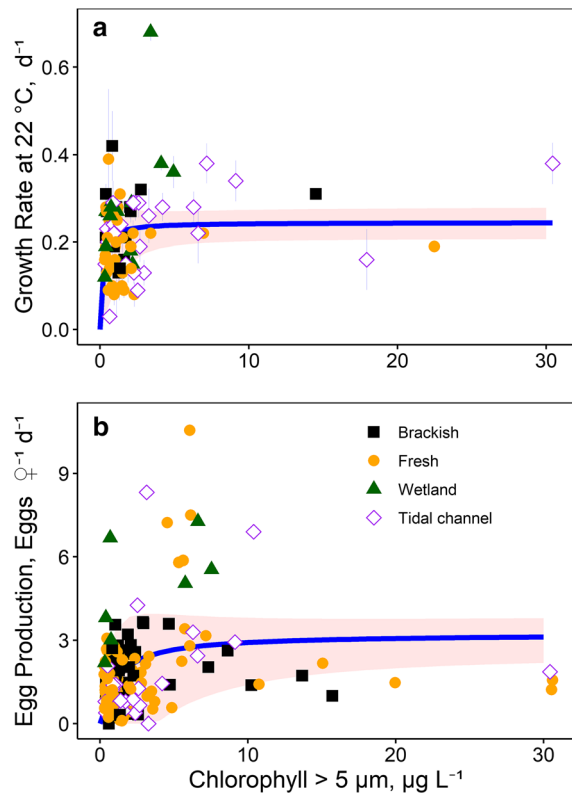
Fig. 8 *Pseudodiaptomus forbesi* vital rates as functions of Chl $a > 5$ μm: **a**, copepodite growth rate (d^{-1}) adjusted to 22 °C; **b**, production rate. Blue line is a rectangular hyperbola fitted to the data (Eqs. 1 and 2). Shading as in Fig. 5. Parameters in Table 3. Note that Chl $a > 5$ μm was not measured as often as whole Chl a (Figs. 5 and 7)

needed ∼ 12 h to convert food to eggs (Tester and Turner 1990) and females of demersal *Pseudodiaptomus* species integrate over even longer periods (Fancett and Kimmerer 1985).

Finally, the age structure of the females introduces bias to the egg production rate estimated by the egg-ratio method. *Pseudodiaptomus forbesi* females produce their first clutch ∼ 2 d or more after molting from copepodite stage 5 (Kimmerer et al. 2018b). Since young, pre-reproductive females are indistinguishable from females that are between clutches, the egg production rate will be biased low when a large fraction of the females is pre-reproductive regardless of the available nutrition. Females may also become less fecund as they age. Since mortality rate controls the age structure, Ohman et al. (1996) recommended correcting calculated egg production rates for mortality. We lack the data to correct these rates, although
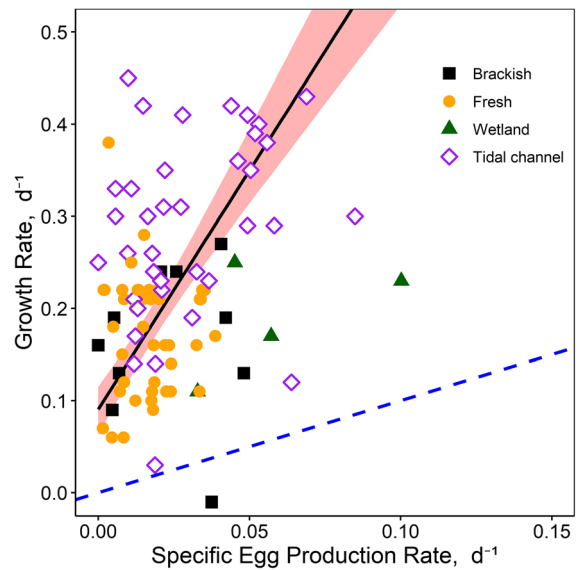
Fig. 9 *Pseudodiaptomus forbesi* copepodite growth rate (d^{-1}) as a function of female specific egg production rate (SEPR, d^{-1}; $N = 100$). Black line is a geometric mean regression with shaded area showing approximate 95% confidence interval, and dashed line is 1:1

mortality of female *P. forbesi* in our study area can be high (Kimmerer et al. 2019).

Of the above impediments to a good predictive model of copepod growth and reproduction, the first two could be improved by the use of better proxies for food than Chl a. However, there is some inconsistency among studies using alternative proxies, revealing subtleties in the description of the foods of copepods. These subtleties include a divergence in nutritional requirements between copepodites and adults, as demonstrated by elevated EPR but not growth of two copepod species fed a mixed diet instead of a single phytoplankton species (Koski et al. 2006). Essential fatty acids and particulate organic carbon and nitrogen have all shown strong relationships to copepod growth and EPR (Houde and Roman 1987; Jónasdóttir et al. 1995). EPR of *Acartia hudsonica* in Long Island Sound, USA, was highly correlated with fatty acid composition of the seston (Jónasdóttir et al. 1995), and this relationship was linked to Chl a and abundance of ciliates. *Calanus helgolandicus* EPR was also strongly correlated with fatty acid composition, but not with Chl a, particulate carbon, or nitrogen (Pond et al. 1996). Our limited results using LCEFA % as a predictor contrast with the above results, in that the fit to growth rate was no better than that using Chl a as a
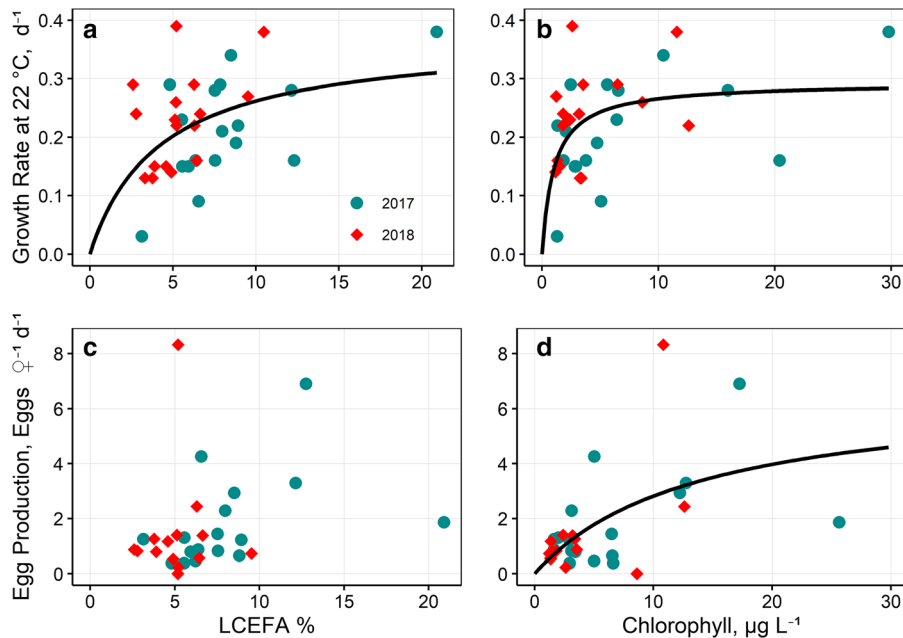
Fig. 10 *Pseudodiaptomus forbesi*: **a, b** copepodite growth rates adjusted to 22 °C; **c, d** egg production rates vs. percent LCEFA in total lipids (LCEFA %, **a, c**) and whole Chl *a* concentration (**b, d**). Lines show fits of Eqs. 1 or 2 (substituting LCEFA % for chlorophyll in a and c), except that no line could be fitted to data in panel **c**

predictor, and there was no relationship between LCEFA % and EPR (Fig. 10).

More broadly, nutrition and its support of the growth of copepods and other aquatic organisms is more complicated than implied by any single proxy for food (Anderson and Hessen 1995; Anderson et al. 2020). Correlations among attributes of the food environment may obscure the strength of relationships, particularly when the attributes are measured to different degrees of precision. Further, copepod food is unevenly distributed in aquatic environments, particularly in estuaries with their gradients and sub-habitats. In the open waters of the SFE, where Chl *a* was almost always low, *P. forbesi* EPR was predominantly low (Fig. 7). The wetland and tidal channel have long residence times (Gross et al. 2019), isolating these habitats from the open waters. This spatial decoupling of temporal variability in chlorophyll concentration and associated foodweb productivity allows for accumulation of phytoplankton biomass, resulting in frequent elevation of copepod growth rates above those in the open waters.

Reproduction and growth of sac-spawning copepods

The two reproductive strategies of copepods, broadcasting and sac-spawning, affect both copepodite growth (Liu and Hopcroft 2008) and female reproduction: sac-spawning females commonly have higher egg hatching success and lower egg mortality and often produce fewer eggs than broadcast spawners (Kiørboe and Sabatini 1995). Our estimates of EPR for *P. forbesi* averaged $\sim$ 2 eggs $\female^{-1}$ d^{-1} (Table 5). Estimates of EPR of other *Pseudodiaptomus* spp. are not common. Two *Pseudodiaptomus* spp. collected from Westernport Bay, Australia, had an average EPR of 2 eggs $\female^{-1}$ d^{-1} and a maximum of $\sim$ 6 eggs $\female^{-1}$ d^{-1} from laboratory experiments (Fancett and Kimmerer 1985). In the Inland Sea of Japan, *P. marinus* EPR averaged 12 eggs $\female^{-1}$ d^{-1} (Liang and Uye 1997). In the Kariega Estuary, South Africa, *P. hessei* EPR averaged 20 eggs $\female^{-1}$ d^{-1} with a maximum of 37 eggs $\female^{-1}$ d^{-1} over a full year, among the highest EPR values reported for any sac-spawning copepod (Noyon and Froneman 2013).

The sac spawner *Eurytemora carolleeae* (a member of the *E. affinis* complex, Alekseev and Souissi 2011)

has been abundant in the SFE only during winter–spring since the introduction of *Potamocorbula amurensis* (Kimmerer et al. 2014b). The 2006–2007 study determined growth rate and EPR of *E. carolleeae* during late spring, reporting a mean EPR of only 3 eggs $♀^{-1}$ d^{-1}, similar to that of *P. forbesi* in the same habitats in summer (Kimmerer et al. 2014b). EPR of *E. carolleeae* collected from Chesapeake Bay was not limited by food (Lloyd et al. 2013), and females cultured in the laboratory had a mean EPR of 38 eggs $♀^{-1}$ d^{-1} (Devreker et al. 2012). Another member of the *E. affinis* species complex collected from Lake Biwa, Japan and cultured in the laboratory had an average EPR of 34 eggs $♀^{-1}$ d^{-1} (Ban 1994). Combining results for *Eurytemora* spp. and *Pseudodiaptomus* spp., it is apparent that reproductive strategy and life history do not fully explain apparent differences in reproductive rates among sac-spawning copepod species or populations.

Somatic growth rates of sac-spawning species are also generally lower than those of broadcast-spawning species (Hirst and Bunker 2003; Liu and Hopcroft 2008). Using growth rates from the literature on copepodites of five sac-spawning taxa adjusted to 15 °C, Hirst and Bunker (2003) fitted growth rate to a rectangular hyperbola with Chl *a* as predictor and obtained a maximum growth (g_{max}) of 0.15 d^{-1}. The g_{max} of *P. forbesi* in our study, determined by fitting Eq. 1 after adjusting growth rates to 15 °C, was similar at 0.16 ± 0.02 d^{-1} (Table 3). The Chl *a* at half-saturation of growth (K_g) estimated by Hirst and Bunker (2003) was 0.02 μg Chl $a·L^{-1}$, much lower than our estimated K_g of 1.6 (0.9, 2.6) μg Chl $a·L^{-1}$ at 15 °C (Table 3). This apparent difference in estimated half-saturation constants suggests that *P. forbesi* may be more susceptible to food limitation than other sac-spawning copepods. Many of the sac-spawning species included in the analysis by Hirst and Bunker (2003) were from the genera *Oithona* and *Pseudocalanus*—the former is an ambush-feeding cyclopoid that consumes motile prey such as ciliates and flagellates (Sabatini and Kiørboe 1994), whereas the latter uses a feeding current to consume both phytoplankton and motile prey (Corkett and McLaren 1978). *Oithona* vital rates may be less comparable to those of *P. forbesi* or other calanoid sac spawners because of *Oithona*'s behavior as an ambush predator, and its diet of mainly motile prey may dissociate growth from phytoplankton biomass. The K_g

estimated by Hirst and Bunker (2003) for three species of *Pseudocalanus* combined was 0.8 μg Chl $a·L^{-1}$, a value much closer to our estimated K_g for *P. forbesi*. Last, the confidence limits for K_g values are typically wide (e.g., our Table 3 and Table 3 in Hirst and Bunker 2003), largely as a consequence of covariation between K_g and g_{max} as discussed above.

Food-saturated somatic growth rate of *P. forbesi* in the laboratory was slightly higher in early copepodite stages (C1–C3, 0.51 ± 0.05 d^{-1}) than in later stages (C4–C5, 0.45 ± 0.06 d^{-1}, Kimmerer et al. 2018b). In our study, growth rate of early copepodites in the field was weakly correlated with, and much higher than, SEPR ($r = 0.28$, Fig. 9). These results seem to follow the general pattern of declining growth rate in later life stages of calanoid copepods under both food-saturated and food-limited conditions (Vidal 1980). Although copepodite growth rate and SEPR can be similar when neither is food limited (Berggreen et al. 1988; Fryd et al. 1991), they may diverge under field conditions or when food is limiting (Peterson et al. 1991; Hopcroft and Roff 1998; Richardson and Verheye 1998). Five dominant calanoid copepods in the Skagerrak had an average copepodite growth rate of 0.27 d^{-1} compared to an average SEPR of 0.1 d^{-1} (Peterson et al. 1991). In a tropical system, copepodite growth rates were higher than SEPR of female copepods with carbon contents greater than 3.5 μg C per individual (Hopcroft and Roff 1998). And our results show a wide gap between somatic growth rate and SEPR (Fig. 9). These differences may indicate that adult females have different nutritional needs than copepodites and therefore may need a more diverse diet to support egg production than is needed by copepodites for growth (Koski et al. 2006). In contrast, in the Alboran Sea with low phytoplankton biomass (< 3 μg Chl $a·L^{-1}$), naupliar growth rates of *Centropages typicus* were mostly lower than SEPR, suggesting food limitation in the earliest stages (Calbet et al. 2000). Altogether, the principal mechanisms that drive the observed differences between growth rate of developing life stages and SEPR are related to life history, physiology, and the way that food limitation affects individual stages.

Pelagic habitat in estuaries

Estuaries are often considered highly productive (Ketchum 1967), but the diversity of estuarine systems

and the focus of much research on single estuaries have limited the development of general paradigms about pelagic productivity in estuaries. Recent syntheses have shown phytoplankton productivity to be extremely variable within and among estuaries because of their complex connections to land, ocean, and atmosphere, interactions between plankton and benthos, and modification by humans (Cloern and Jassby 2008, 2010; Cloern et al. 2014). In many estuaries, high turbidity from land runoff and wind-wave resuspension attenuates light, restricting the depth over which net growth of phytoplankton is possible. Most of the northern SFE is an unproductive environment where turbidity restricts light available to support phytoplankton growth in deep channels, benthic grazing limits accumulation of phytoplankton biomass, and tidal mixing limits residence time in productive areas (Cole and Cloern 1987; Lucas and Thompson 2012; Kimmerer and Thompson 2014).

Shallow areas can be more productive than deep areas because light penetrates through a greater fraction of the water column, and water residence times can be longer than in deep channels. For example, satellite image data revealed higher Chl a in the tributaries of Chesapeake Bay than in the main channels (Abbas et al. 2019). However, the high surface/volume ratio in shallow areas amplifies the effect of benthic grazing in constraining blooms (Lucas and Thompson 2012). In the Cache Slough Complex of the northern SFE ("wetland," Fig. 1), high Chl a values are associated with long water residence times (Downing et al. 2016; Gross et al. 2019). During winter floods in the Yolo Bypass, short residence time and high turbidity limit the accumulation of phytoplankton biomass; however, as flood waters recede, residence times and water clarity increase, and phytoplankton blooms can occur (Schemel et al. 2004). During the dry season, the Yolo Bypass is confined to a narrow tidal channel and phytoplankton can bloom, especially when flow pulses provide nutrients to sustain growth (Frantzich et al. 2018). Finally, phytoplankton blooms arising in a tributary channel can elevate phytoplankton biomass in main channels where conditions are unconducive to bloom (Jungbluth et al. 2020).

From Eqs. 1 and 2, the chlorophyll a concentration where growth or EPR is 90% of the maximum is 9 times the half-saturation constant K. This is ~ 16 µg Chl $a \cdot L^{-1}$ for growth, which was exceeded in 9% of the measurements, and 26 µg Chl $a \cdot L^{-1}$ for EPR, which was exceeded in 2% of the measurements. From long-term monitoring data since 1987, Chl a has exceeded 16 µg Chl $a \cdot L^{-1}$ infrequently in main channels of the northern SFE, except in the southeastern Delta where residence time is long (Jassby 2008). This implies that food limitation of zooplankton is chronic and persistent in much of the northern estuary, except in some shallow areas where phytoplankton biomass may accumulate. Bioassay experiments with the cladoceran *Daphnia magna,* using water from sites in the same general area as our study, showed a strong relationship of growth rate to Chl a with a half-saturation constant of ~ 2.5 µg Chl $a \cdot L^{-1}$ (estimated from Fig. 3 of Müller-Solger et al. 2002). By using cultured bioassay organisms, the researchers eliminated several of the sources of confounding variability discussed above, but the point of saturation for growth rate was not very different from that for *P. forbesi* (Table 3).

Thus, shallow peripheral habitats may provide areas of higher zooplankton production that support foraging by pelagic fishes (Sommer and Mejia 2013; Hammock et al. 2017). However, in the SFE these areas are small and their contribution to the overall productivity of the estuary must also be small (Jassby and Cloern 2000). These habitats have attracted the interest of managers who seek ways to reverse declines in native fishes. Peripheral habitats are the focus of study for two reasons: 1) to enhance understanding of food webs supporting fishes of concern, and 2) as guides for large-scale restoration projects (Herbold et al. 2014). The endangered delta smelt *Hypomesus transpacificus* continues to decline in abundance, partly because its copepod prey is in short supply (Sommer and Mejia 2013). Although the usual spring–autumn habitat of delta smelt is brackish open water, a contingent of this population occupies the Cache Slough Complex year-round, possibly trading off stressful temperature and salinity conditions for higher availability of copepods than in their brackish habitat (Sommer and Mejia 2013; Hammock et al. 2017).

Our research shows that copepod vital rates in this region are often elevated partly because of higher phytoplankton biomass. The keys to designing large-scale restoration projects for the purpose of supporting pelagic fishes are: (1) to establish conditions inhibiting settlement of benthic grazers and thereby favorable for

accumulation of phytoplankton biomass (Lucas and Thompson 2012) supporting higher zooplankton growth; (2) to create or restore wetlands large enough to make a substantial contribution to system productivity; and (3) to establish conditions under which the fishes of concern can gain access to this food source.

Summary

The copepod *P. forbesi* is persistently food-limited in the northern SFE, with periods of high growth and reproductive rates in response to elevated phytoplankton biomass as indicated by chlorophyll *a* concentration. Both growth rate and egg production rate had positive, saturating responses to Chl *a*; although only $\sim$ 1/4 of the variance was explained by the model fits, a better relationship can probably be realized only in laboratory studies. Egg production varied among habitats in its response to Chl *a*, with elevated EPR values in the wetland. SEPR was weakly related to, and much lower than, copepodite growth rate. Therefore, both measures are required for a full assessment of copepod productivity. In peripheral habitats of the SFE, copepod growth and female egg production were periodically high in response to elevated phytoplankton biomass, which may support the use of these habitats by pelagic fishes.

Availability of data and material Data can be obtained from the corresponding author upon request.

Declarations

Conflict of interest The authors declare that they have no conflict of interest.

References

Abbas MM, Melesse AM, Scinto LJ, Rehage JS (2019) Satellite estimation of chlorophyll-a using moderate resolution imaging spectroradiometer (MODIS) sensor in shallow coastal water bodies: validation and improvement. Water (Switzerland). https://doi.org/10.3390/w11081621

Akaike H (1974) A new look at the statistical model identification. IEEE Trans Autom Control 19:716–723. https://doi.org/10.1109/TAC.1974.1100705

Alcaraz M, Saiz E, Calbet A, Trepat I, Broglio E (2003) Estimating zooplankton biomass through image analysis. Mar Biol 143:307–315. https://doi.org/10.1007/s00227-003-1094-8

Alekseev VR, Souissi A (2011) A new species within the *Eurytemora affinis* complex (*Copepoda*: *Calanoida*) from the Atlantic Coast of USA, with observations on eight morphologically different European populations. Zootaxa 2767:41–56

Alpine AE, Cloern JE (1992) Trophic interactions and direct physical effects control phytoplankton biomass and production in an estuary. Limnol Oceanogr 37:946–955. https://doi.org/10.4319/lo.1992.37.5.0946

Anderson TR, Hessen DO (1995) Carbon or nitrogen limitation in marine copepods? J Plankton Res 17:317–331. https://doi.org/10.1093/plankt/17.2.317

Anderson TR, Raubenheimer D, Hessen DO, Jensen K, Gentleman WC, Mayor DJ (2020) Geometric stoichiometry: unifying concepts of animal nutrition to understand how protein-rich diets can be "too much of a good thing." Front Ecol Evol. https://doi.org/10.3389/fevo.2020.00196

Arar EJ, Collins GB (1997) Method 445.0 In vitro determination of chlorophyll a and pheophytin in marine and freshwater algae by fluorescence. US Environmental Protection Agency, Washington, DC

Ban S (1994) Effect of temperature and food concentration on post-embryonic development, egg production and adult body size of calanoid copepod *Eurytemora affinis*. J Plankton Res 16:721–735. https://doi.org/10.1093/plankt/16.6.721

Berggreen U, Hansen B, Kiørboe T (1988) Food size spectra, ingestion and growth of the copepod *Acartia tonsa* during development: implications for determination of copepod production. Mar Biol 99:341–352. https://doi.org/10.1007/BF02112126

Bouley P, Kimmerer WJ (2006) Ecology of a highly abundant, introduced cyclopoid copepod in a temperate estuary. Mar Ecol Prog Ser 324:219–228. https://doi.org/10.3354/meps324219

Bowen A, Rollwagen-Bollens G, Bollens SM, Zimmerman J (2015) Feeding of the invasive copepod *Pseudodiaptomus forbesi* on natural microplankton assemblages within the lower Columbia River. J Plankton Res 37:1089–1094. https://doi.org/10.1093/plankt/fbv078

Brylinski JM, Antajan E, Raud T, Vincent D (2012) First record of the Asian copepod *Pseudodiaptomus marinus* Sato, 1913 (*Copepoda*: *Calanoida*: Pseudodiaptomidae) in the southern bight of the North Sea along the coast of France. Aquat Invasions 7:577–584. https://doi.org/10.3391/ai.2012.7.4.014

Bunker A, Hirst A (2004) Fecundity of marine planktonic copepods: global rates and patterns in relation to chlorophyll a, temperature, and body weight. Mar Ecol Prog Ser 279:161–181. https://doi.org/10.3354/meps279161

Calbet A, Trepat I, Arin L (2000) Naupliar growth versus egg production in the calanoid copepod *Centropages typicus*. J Plankton Res 22:1393–1402. https://doi.org/10.1093/plankt/22.7.1393

Checkley DM (1980) The egg production of a marine planktonic copepod in relation to its food supply: laboratory studies. Limnol Ocean 25:430–446. https://doi.org/10.4319/lo.1980.25.3.0430

Cloern JE, Jassby AD (2008) Complex seasonal patterns of primary producers at the land-sea interface. Ecol Lett 11:1294–1303. https://doi.org/10.1111/j.1461-0248.2008.01244.x

Cloern JE, Jassby AD (2010) Patterns and scales of phytoplankton variability in estuarine–coastal ecosystems. Estuaries Coasts 33:230–241. https://doi.org/10.1007/s12237-009-9195-3

Cloern JE, Jassby AD (2012) Drivers of change in estuarine-coastal ecosystems: discoveries from four decades of study in San Francisco Bay. Rev Geophys 50:1–33. https://doi.org/10.1029/2012RG000397

Cloern JE, Foster SQ, Kleckner AE (2014) Phytoplankton primary production in the world's estuarine-coastal ecosystems. Biogeosciences 11:2477–2501. https://doi.org/10.5194/bg-11-2477-2014

Cole BE, Cloern JE (1987) An empirical model for estimating phytoplankton productivity in estuaries. Mar Ecol Prog Ser 36:299–305

Corkett CJ, McLaren IA (1978) The biology of *Pseudocalanus*. Adv Mar Biol 15:1–231

Dege M, Brown LR (2004) Effect of outflow on spring and summertime distribution and abundance of larval and juvenile fishes in the upper San Francisco Estuary. In: Feyrer F, Brown LR, Brown RL, Orsi JJ (eds) Symp. Early life history of fishes in the San Francisco Estuary and watershed. American Fisheries Society, Bethesda MD, pp 49–65

Devreker D, Pierson JJ, Souissi S, Kimmel DG, Roman MR (2012) An experimental approach to estimate egg production and development rate of the calanoid copepod *Eurytemora affinis* in Chesapeake Bay, USA. J Exp Mar Bio Ecol 416:72–83. https://doi.org/10.1016/j.jembe.2012.02.010

Downing BD, Bergamaschi BA, Kendall C, Kraus TEC, Dennis KJ, Carter JA, Von Dessonneck TS (2016) Using continuous underway isotope measurements to map water residence time in hydrodynamically complex tidal environments. Environ Sci Technol 50:13387–13396. https://doi.org/10.1021/acs.est.6b05745

Edmondson W, Comita GW, Anderson GC (1962) Reproductive rate of copepods in nature and its relation to phytoplankton population. Ecology 43:625–634

Eppley RW, Sloan PR (1966) Growth rates of marine phytoplankton: correlation with light absorption by cell chlorophyll a. Physiol Plant 19:47–59. https://doi.org/10.1111/j.1399-3054.1966.tb09073.x

Fancett M, Kimmerer W (1985) Vertical migration of the demersal copepod *Pseudodiaptomus* as a means of predator avoidance. J Exp Mar Bio Ecol 88:31–43

Frantzich J, Sommer T, Schreier B (2018) Physical and biological responses to flow in a tidal freshwater slough complex. San Franc Estuary Watershed Sci. https://doi.org/10.15447/sfews.2018v16iss1/art3

Fryd M, Haslund OH, Wohlgemuth O (1991) Development, growth and egg production of the two copepod species *Centropages hamatus* and *Centropages typicus* in the laboratory. J Plankton Res 13:683–689. https://doi.org/10.1093/plankt/13.4.683

Galloway AWE, Winder M (2015) Partitioning the relative importance of phylogeny and environmental conditions on phytoplankton fatty acids. PLoS One. https://doi.org/10.1371/journal.pone.0130053

Ger KA, Otten TG, DuMais R, Ignoffo T, Kimmerer W (2018) In situ ingestion of *Microcystis* is negatively related to copepod abundance in the upper San Francisco Estuary. Limnol Oceanogr 1999:2394–2410. https://doi.org/10.1002/lno.10946

Gross E, Andrews S, Bergamaschi B, Downing B, Holleman R, Burdick S, Durand J (2019) The use of stable isotope-based water age to evaluate a hydrodynamic model. Water (Switzerland). https://doi.org/10.3390/w11112207

Hammock BG, Slater SB, Baxter RD, Fangue NA, Cocherell D, Hennessy A, Kurobe T, Tai CY, Teh SJ (2017) Foraging and metabolic consequences of semi-anadromy for an endangered estuarine fish. PLoS ONE 12:1–25. https://doi.org/10.1371/journal.pone.0173497

Herbold B, Baltz DM, Brown L, Grossinger R, Kimmerer W, Lehman P, Simenstad CS, Wilcox C, Nobriga M (2014) The role of tidal marsh restoration in fish management in

the San Francisco Estuary. San Franc Estuary Watershed Sci. https://doi.org/10.15447/sfews.2014v12iss1art1

Hirst A, Bunker A (2003) Growth of marine planktonic copepods: global rates and patterns in relation to chlorophyll a, temperature, and body weight. Limnol Oceanogr 48:1988–2010. https://doi.org/10.4319/lo.2003.48.5.1988

Hirst AG, Keister JE, Richardson AJ, Ward P, Shreeve RS, Escribano R (2014) Re-assessing copepod growth using the Moult Rate method. J Plankton Res 36:1224–1232. https://doi.org/10.1093/plankt/fbu045

Hopcroft R, Roff J (1998) Zooplankton growth rates: the influence of female size and resources on egg production of tropical marine copepods. Mar Biol 132:79–86. https://doi.org/10.1007/s002270050373

Houde S, Roman M (1987) Effects of food quality on the functional ingestion response of the copepod *Acartia tonsa*. Mar Ecol Prog Ser 40:69–77. https://doi.org/10.3354/meps040069

Jassby AD (2008) Phytoplankton in the upper San Francisco Estuary: recent biomass trends, their causes, and their trophic significance. San Franc Estuary Watershed Sci. https://doi.org/10.15447/sfews.2008v6iss1art2

Jassby AD, Cloern JE (2000) Organic matter sources and rehabilitation of the Sacramento-San Joaquin Delta (California, USA). Aquat Conserv Mar Freshw Ecosyst 10:323–352. https://doi.org/10.1002/1099-0755(200009/10)10:5%3c323::AID-AQC417%3e3.0.CO;2-J

Jónasdóttir SH, Fields D, Pantoja S (1995) Copepod egg production in Long Island Sound, USA, as a function of the chemical composition of seston. Mar Ecol Prog Ser 119:87–98. https://doi.org/10.3354/meps119087

Jungbluth MC, Lee C, Patel C, Ignoffo T, Bergamaschi B, Kimmerer W (2020) Production of the copepod *Pseudodiaptomus forbesi* is not enhanced by ingestion of the diatom *Aulacoseira granulata* during a bloom. Estuaries Coasts. https://doi.org/10.1007/s12237-020-00843-9

Kayfetz KR, Kimmerer WJ (2017) Abiotic and biotic controls on the copepod *Pseudodiaptomus forbesi* in the upper San Francisco Estuary. Mar Ecol Prog Ser 581:85–101. https://doi.org/10.3354/meps12294

Ketchum BH (1967) Phytoplankton nutrients in estuaries. In: Lauff GH (ed) Estuaries. American Association for the Advancement of Science, Washington D.C., pp 329–335

Kimmel DG (2012) Plankton consumer groups: copepods. In: Wolanski E, McLusky DS (eds) Treatise on Estuarine and coastal science. Academic Press, Waltham, pp 95–126

Kimmerer WJ (2004) Open water processes of the San Francisco Estuary: from physical forcing to biological responses. San Franc Estuary Watershed Sci. https://doi.org/10.5811/westjem.2011.5.6700

Kimmerer WJ, McKinnon AD (1986) Glutaraldehyde fixation to maintain biomass of preserved plankton. J Plankton Res 8:1003–1008. https://doi.org/10.1093/plankt/8.5.1003

Kimmerer WJ, McKinnon AD (1987) Growth, mortality, and secondary production of the copepod *Acartia tranteri* in Westernport Bay, Australia. Limnol Oceanogr 32:14–28. https://doi.org/10.4319/lo.1987.32.1.0014

Kimmerer WJ, Slaughter AM (2016) Fine-scale distributions of zooplankton in the northern San Francisco Estuary. San Franc Estuary Watershed Sci. https://doi.org/10.5811/westjem.2011.5.6700

Kimmerer WJ, Thompson JK (2014) Phytoplankton growth balanced by clam and zooplankton grazing and net transport into the low-salinity zone of the San Francisco Estuary. Estuaries Coasts 37:1202–1218. https://doi.org/10.1007/s12237-013-9753-6

Kimmerer W, Burau J, Bennett W (2002) Persistence of tidally-oriented vertical migration by zooplankton in a temperate estuary. Estuaries 25:359–371. https://doi.org/10.1007/BF02695979

Kimmerer WJ, Hirst AG, Hopcroft RR, McKinnon AD (2007) Estimating juvenile copepod growth rates: corrections, inter-comparisons and recommendations. Mar Ecol Prog Ser 336:187–202. https://doi.org/10.3354/meps336187

Kimmerer WJ, Parker AE, Lidström UE, Carpenter EJ (2012) Short-term and interannual variability in primary production in the Low-Salinity Zone of the San Francisco Estuary. Estuaries Coasts 35:913–929. https://doi.org/10.1007/s12237-012-9482-2

Kimmerer WJ, Gross ES, MacWilliams ML (2014a) Tidal migration and retention of estuarine zooplankton investigated using a particle-tracking model. Limnol Oceanogr 59:901–906. https://doi.org/10.4319/lo.2014.59.3.0901

Kimmerer WJ, Ignoffo TR, Slaughter AM, Gould AL (2014b) Food-limited reproduction and growth of three copepod species in the low-salinity zone of the San Francisco Estuary. J Plankton Res 36:722–735. https://doi.org/10.1093/plankt/fbt128

Kimmerer WJ, Ignoffo TR, Kayfetz KR, Slaughter AM (2018) Effects of freshwater flow and phytoplankton biomass on growth, reproduction, and spatial subsidies of the estuarine copepod *Pseudodiaptomus forbesi*. Hydrobiologia 807:113–130. https://doi.org/10.1007/s10750-017-3385-y

Kimmerer W, Ignoffo TR, Bemowski B, Moderan J, Holmes A, Bergamaschi B (2018) Zooplankton dynamics in the Cache Slough Complex of the upper San Francisco Estuary. San Franc Estuary Watershed Sci. https://doi.org/10.15447/sfews.2018v16iss3art4

Kimmerer WJ, Gross ES, Slaughter AM, Durand JR (2019) Spatial subsidies and mortality of an estuarine copepod revealed using a box model. Estuaries Coasts 42:218–236. https://doi.org/10.1007/s12237-018-0436-1

Kiørboe T (1993) Turbulence, phytoplankton cell size, and the structure of pelagic food webs. Adv Mar Biol 29:1–72

Kiørboe T (1998) Population regulation and role of mesozooplankton in shaping marine pelagic food webs. Hydrobiologia 363:13–27. https://doi.org/10.1023/A:1003173721751

Kiørboe T, Sabatini M (1995) Scaling of fecundity, growth and development in marine planktonic copepods. Mar Ecol Prog Ser 120:285–298. https://doi.org/10.3354/meps120285

Kleppel G, Davis CS, Carter K (1996) Temperature and copepod growth in the sea: a comment on the temperature-dependent model of Huntley and Lopez. Am Nat 148:397–406

Kobari T, Sastri AR, Yebra L, Liu H, Hopcroft RR (2019) Evaluation of trade-offs in traditional methodologies for measuring metazooplankton growth rates: assumptions, advantages and disadvantages for field applications. Prog Oceanogr 178:102137. https://doi.org/10.1016/j.pocean.2019.102137

Koski M, Klein Breteler W, Schogt N, Gonzalez S, Jakobsen HH (2006) Life-stage-specific differences in exploitation of food mixtures: diet mixing enhances copepod egg production but not juvenile development. J Plankton Res 28:919–936. https://doi.org/10.1093/plankt/fbl029

Liang D, Uye S (1997) Population dynamics and production of the planktonic copepods in a eutrophic inlet of the Inland Sea of Japan. IV. *Pseudodiaptomus marinus*, the egg-carrying calanoid. Mar Biol 128:415–421. https://doi.org/10.1007/s002270050107

Liu H, Hopcroft RR (2008) Growth and development of *Pseudocalanus* spp. in the northern Gulf of Alaska. J Plankton Res 30:923–935. https://doi.org/10.1093/plankt/fbn046

Lloyd SS, Elliott DT, Roman MR (2013) Egg production by the copepod, *Eurytemora affinis*, in Chesapeake Bay turbidity maximum regions. J Plankton Res 35:299–308. https://doi.org/10.1093/plankt/fbt003

Lucas LV, Thompson JK (2012) Changing restoration rules: exotic bivalves interact with residence time and depth to control phytoplankton productivity. Ecosphere 3(12):1–26. https://doi.org/10.1890/ES12-00251.1

McLaren IA (1965) Some relationships between temperature and egg size, body size, development rate, and fecundity, of the copepod *Pseudocalanus*. Limnol Oceanogr 10:528–538. https://doi.org/10.4319/lo.1965.10.4.0528

Morgan-King TL, Schoellhamer DH (2013) Suspended-sediment flux and retention in a backwater tidal slough complex near the landward boundary of an estuary. Estuaries Coasts 36:300–318. https://doi.org/10.1007/s12237-012-9574-z

Müller-Solger AB, Jassby AD, Müller-Navarra DC (2002) Nutritional quality of food resources for zooplankton (*Daphnia*) in a tidal freshwater system (Sacramento-San Joaquin River Delta). Limnol Oceanogr 47:1468–1476. https://doi.org/10.4319/lo.2002.47.5.1468

Nichols FH, Cloern JE, Luoma SN, Peterson DH (1986) The modification of an estuary. Science 231:567–573. https://doi.org/10.1126/science.231.4738.567

Nixon SW, Oviatt CA, Frithsen J, Sullivan B (1986) Nutrients and the productivity of estuarine and coastal marine systems. J Limnol Soc Sth Afr 12:43–71. https://doi.org/10.1080/03779688.1986.9639398

Noyon M, Froneman PW (2013) Variability in the egg production rates of the calanoid copepod, *Pseudodiaptomus hessei* in a South African estuary in relation to environmental factors. Estuar Coast Shelf Sci 135:306–316. https://doi.org/10.1016/j.ecss.2013.10.024

Ohman MD, Aksnes DL, Runge JA (1996) The interrelationship of copepod fecundity and mortality. Limnol Oceanogr 41:1470–1477. https://doi.org/10.4319/lo.1996.41.7.1470

Orsi J, Mecum W (1986) Zooplankton distribution and abundance in the Sacramento-San Joaquin Delta in relation to certain environmental factors. Estuaries 9:326–339

Orsi JJ, Walter TC (1991) *Pseudodiaptomus forbesi* and *P. marinus* (*Copepoda*: *Calanoida*), the latest copepod immigrants to California's Sacramento-San Joaquin Estuary. Proc Fourth Int Conf Copepoda 553–561

Owens S, Ignoffo TR, Frantzich J, Slaughter A, Kimmerer W (2019) High growth rates of a dominant calanoid copepod in the northern San Francisco Estuary. J Plankton Res 41:939–954. https://doi.org/10.1093/plankt/fbz064

Parker AE, Dugdale RC, Wilkerson FP (2012) Elevated ammonium concentrations from wastewater discharge depress primary productivity in the Sacramento River and the northern San Francisco Estuary. Mar Pollut Bull 64:574–586. https://doi.org/10.1016/j.marpolbul.2011.12.016

Parrish CC (2013) Lipids in marine ecosystems. ISRN Oceanogr. https://doi.org/10.5402/2013/604045

Peterson WT, Tiselius P, Kiørboe T (1991) Copepod egg production, moulting and growth rates, and secondary production, in the Skagerrak in August 1988. J Plankton Res 13:131–154. https://doi.org/10.1093/plankt/13.1.131

Pond D, Harris R, Head R, Harbour D (1996) Environmental and nutritional factors determining seasonal variability in the fecundity and egg viability of *Calanus helgolandicus* in coastal waters off Plymouth, UK. Mar Ecol Prog Ser 143:45–63. https://doi.org/10.3354/meps143045

R Core Team (2020) R: A language and environment for statistical computing. R Foundation for Statistical Computing, Vienna, Austria

Richardson AJ, Verheye HM (1998) The relative importance of food and temperature to copepod egg production and somatic growth in the southern Benguela upwelling system. J Plankton Res 20:2379–2399. https://doi.org/10.1093/plankt/20.12.2379

Ricker WE (1973) Linear regression in fishery research. J Fish Res Bd Canada 30:409–434

Runge JA, Roff JC (2000) The measurement of growth and reproductive rates. In: Harris RP, Wiebe PH, Lenz J, Skjoldal HR, Huntley M (eds) ICES Zooplankton methodology manual. Academic Press, San Diego, CA, pp 401–454

Sabatini M, Kiørboe T (1994) Egg production, growth and development of the cyclopoid copepod *Oithona similis*. J Plankton Res 16:1329–1351. https://doi.org/10.1093/plankt/16.10.1329

Saiz E, Calbet A (2011) Copepod feeding in the ocean: scaling patterns, composition of their diet and the bias of estimates due to microzooplankton grazing during incubations. Hydrobiologia 666:181–196. https://doi.org/10.1007/s10750-010-0421-6

Schemel LE, Sommer TR, Müller-Solger AB, Harrell WC (2004) Hydrologic variability, water chemistry, and phytoplankton biomass in a large floodplain of the Sacramento River, CA. USA Hydrobiologia 513(1–3):129–139. https://doi.org/10.1023/B:hydr.0000018178.85404.1c

Sekiguchi H, McLaren I, Corkett C (1980) Relationship between growth rate and egg production in *Acartia clausi hudsonica*. Mar Biol 58:133–138

Sheaves M, Baker R, Nagelkerken I, Connolly RM (2014) True value of estuarine and coastal nurseries for fish: incorporating complexity and dynamics. Estuaries Coasts 38:401–414. https://doi.org/10.1007/s12237-014-9846-x

Smith EP (2020) Ending reliance on statistical significance will improve environmental inference and communication. Estuaries Coasts 43:1–6. https://doi.org/10.1007/s12237-019-00679-y

Sobczak WV, Cloern JE, Jassby AD, Cole BE, Schraga TS, Arnsberg A (2005) Detritus fuels ecosystem metabolism but not metazoan food webs in San Francisco estuary's

freshwater delta. Estuaries 28:124–137. https://doi.org/10.1007/BF02732759

Sommer T, Mejia F (2013) A place to call home: a synthesis of delta smelt habitat in the upper San Francisco Estuary. San Franc Estuary Watershed Sci. https://doi.org/10.15447/sfews.2013v11iss2art4

Sommer T, Harrell B, Nobriga M, Brown R, Moyle P, Kimmerer W, Schemel L (2001) California's Yolo Bypass: evidence that flood control can be compatible with fisheries, wetlands, wildlife, and agriculture. Fisheries 26:6–16. https://doi.org/10.1577/1548-8446(2001)026%3c0006:CYB%3e2.0.CO;2

Sommer T, Armor C, Baxter R, Breuer R, Brown L, Chotkowski M, Culberson S, Feyrer F, Gingras M, Herbold B, Kimmerer W, Mueller Solger A, Nobriga M, Souza K (2007) The collapse of pelagic fishes in the upper San Francisco Estuary. Fisheries 32:270–277. https://doi.org/10.1577/1548-8446(2007)32[270:TCOPFI]2.0.CO;2

Spiess A-J (2018) propagate: propagation of uncertainty. https://CRAN.R-project.org/package=propagate

Stoecker DK, Egloff DA (1987) Predation by Acartia tonsa Dana on planktonic ciliates and rotifers. J Exp Mar Biol Ecol 110:53–68. https://doi.org/10.1016/0022-0981(87)90066-9

Sullivan LJ, Kimmerer WJ (2013) Egg development times of Eurytemora affinis and Pseudodiaptomus forbesi (Copepoda, Calanoida) from the upper San Francisco Estuary with notes on methods. J Plankton Res 35:1331–1338. https://doi.org/10.1093/plankt/fbt076

Tester PA, Turner JT (1990) How long does it take copepods to make eggs? J Exp Mar Bio Ecol. 141:169–182

Uye S, Sano K (1995) Seasonal reproductive biology of the small cyclopoid copepod Oithona. Mar Ecol Prog Ser 118:121–128. https://doi.org/10.3354/meps171037

Vidal J (1980) Physioecology of zooplankton. I. Effects of phytoplankton concentration, temperature, and body size on the growth rates of Calanus pacificus and Pseudocalanus sp. Mar Biol 56:111–134

Walter TC (1987) Review of the taxonomy and distribution of the demersal copepod genus Pseudodiaptomus (Calanoida: Pseudodiaptomidae) from southern Indo-Pacific waters. Aust J Mar Freshw Res 38:363–396. https://doi.org/10.1071/MF9870363

Wasserstein RL, Lazar NA (2016) The ASA's statement on p-values: context, process, and purpose. Am Stat 70:129–133. https://doi.org/10.1080/00031305.2016.1154108

Whipple AA, Grossinger RM, Rankin D, Stanford B, Askevold RA (2012) Sacramento-San Joaquin Delta historical ecology investigation: Exploring pattern and process. SFEI Contribution No. 672, San Francisco Estuary Institute, Richmond, CA

White JR, Roman MR (1992) Egg production by the calanoid copepod Acartia tonsa in the mesohaline Chesapeake Bay: The importance of food resources and temperature. Mar Ecol Prog Ser 86:239–249

Wickham H (2016) ggplot2: elegant graphics for data analysis. Springer-Verlag, New York

Winder M, Jassby AD (2011) Shifts in zooplankton community structure: implications for food web processes in the Upper San Francisco Estuary. Estuaries Coasts 34:675–690. https://doi.org/10.1007/s12237-010-9342-x

York JK, McManus GB, Kimmerer WJ, Slaughter AM, Ignoffo TR (2014) Trophic links in the plankton in the low salinity zone of a large temperate estuary: top-down effects of introduced copepods. Estuaries Coasts 37:576–588. https://doi.org/10.1007/s12237-013-9698-9